DEPENDENCE OF BORON AND SODIUM IN FLUE GAS FROM A BOROSILICATE GLASS MELTING FURNACE ON OXYGEN TO NATURAL GAS RATIO

Peter M. Walsh, Howard A. Johnsen, and David K. Ottesen

Sandia National Laboratories
Livermore, California

Report prepared for the

CertainTeed Corporation Insulation Group
Blue Bell, Pennsylvania and Chowchilla, California

and the

Glass Manufacturing Industry Council
Westerville, Ohio

Project supported by the

Glass Manufacturing Industry Council

and the

U.S. Department of Energy, Office of Industrial Technologies,
Industries of the Future Glass Team

under the

Glass – Project Laboratory User Services (G+) Program

January 18,2001

CONTENTS

Section	Page
List of Tables	iii
List of Figures	iv
Acknowledgments	v
Introduction	1
Motivation for the Work	1
Laser-Induced Breakdown Spectroscopy (LIBS)	1
Electron Micrograph of the Precipitator Dust	2
Field Work	2
Experimental Measurements and Data Analysis	6
Test Site and Instrumentation	6
Adaptation of LIBS to the Problem	6
Test Program and Procedure	10
Determination of Gas Flow Rate	13
NO_x Emission	14
Spectrum of Light Emitted by Gaseous Species in the Combustion Space	14
Results and Discussion	18
Boron	18
Sodium	24
Conclusions and Recommendations	30
Conclusions	30
Recommendations	31
Nomenclature	32
References	33
Appendix A: Analyses of dust and slag samples	A1
Appendix B: Analyses of the natural gas and the fuel oil used to wet the batch	B1
Appendix C: Computer code for calculation of the flue gas flow rate	C1

LIST OF TABLES

Table | Page

1. Conditions during the Measurements of Boron and Sodium in the Horizontal Flue and at the Electrostatic Precipitator Outlet. 11

2. Relative Concentrations and Mass Flow Rates of Boron in the Horizontal Flue. 19

3. Concentrations and Mass Flow Rates of Boron at the Electrostatic Precipitator Outlet. 22

4. Relative Concentrations and Mass Flow Rates of Sodium in the Horizontal Flue. 25

5. Concentrations and Mass Flow Rates of Sodium at the Electrostatic Precipitator Outlet. 27

LIST OF FIGURES

Figure — Page

1. Schematic diagram of the Sandia laser-induced breakdown spectroscopy (LIBS) instrument, showing the arrangement of the optical system for focusing the laser pulses and collecting the light emitted by the spark. 3

2. Scanning electron micrograph of particles in a dust sample from the electrostatic precipitator collected by Mark Stahl on July 18, 2000. 4

3. Close-up photograph of the LIBS instrument mounted on the duct downstream from the electrostatic precipitator. 7

4. View from the direction opposite to that in Figure 3, of the LIBS equipment at the sampling location downstream from the electrostatic precipitator. 8

5. Typical spectrum obtained by superimposing the individual spectra generated by 1000 laser sparks in the horizontal flue, showing good separation of the boron peak from the carbon and silicon peaks. 9

6. Volumetric flow rates of gas in the horizontal flue and at the electrostatic precipitator outlet as functions of the oxygen to natural gas ratio. 15

7. Nitrogen oxides in the stack gas as a function of the oxygen to natural gas ratio. . 16

8. Example showing the dependence of: a. the boron concentration in flue gas, b. the volumetric flow rate of flue gas, and c. the mass flow rate of boron, on the oxygen to natural gas ratio. 20

9. Dependence of boron mass flow rate in the horizontal flue on oxygen to natural gas ratio. (Same data as shown in Figure 8c.) 21

10. Dependence of boron mass flow rate at the electrostatic precipitator outlet on oxygen to natural gas ratio. 23

11. Dependence of sodium mass flow rate in the horizontal flue on oxygen to natural gas ratio. 26

12. Dependence of sodium mass flow rate at the electrostatic precipitator outlet on oxygen to natural gas ratio. 28

ACKNOWLEDGMENTS

The authors thank the CertainTeed Corporation Insulation Group and workers at the Chowchilla, California, Plant for their generous hospitality and spirit of cooperation throughout all the phases of this project. We especially appreciate the work of Bryon Abshire, Terry L. Berg, Jeffrey T. Curtin, Benjamin M. Dynys, Chris Keran, and Markus H. Stahl, all of whom contributed directly to the success of the measurement campaign.

The authors are also grateful that Sandia National Laboratories was selected by the CertainTeed Corporation and the Glass Manufacturing Industry Council to collaborate in one of the first G+ Program projects. We have found the G+ Program to be an effective mechanism for rapid communication of ideas and technology between the national laboratories and the glass industry.

INTRODUCTION

Motivation for the Work

Volatilization of boron compounds during melting of borosilicate glasses in tank furnaces is a well-known problem associated with the manufacture of glasses having these compositions. While emissions of the particulate matter formed from the volatile species can be controlled by passing the flue gas through an electrostatic precipitator, the problem is complicated by the fact that some boric acids, such as HBO_2 and H_3BO_3, have sufficiently high vapor pressures at gas temperatures typical of a precipitator that a significant fraction of the boron-containing species can pass through the precipitator as vapor, forming particles downstream or in the stack plume, and contributing to particulate emissions and plume opacity (Slade, 1996; J. T. Curtin, personal communications, 2000). At the CertainTeed Corporation insulation plant, where the work described in this report was done, the escape of boric acid vapor species is further reduced by treating the flue gas with aqueous sodium hydroxide in a spray tower upstream from the electrostatic precipitator, promoting conversion of the boric acids to non-volatile sodium metaborate.

CertainTeed engineers were aware, from their experience, that boron emissions and stack plume opacity depended upon the oxygen to natural gas ratio at the burners, tending to decrease as the oxygen to gas ratio was increased. However, increasing the oxygen to gas ratio has the undesirable effect of increasing nitrogen oxides emissions. The objective of the present work was to quantify the dependence of boron in flue gas on stoichiometric ratio, in hopes that better understanding of the process might suggest ways in which the performance of the system could be optimized with respect to both NO_X and particulate emissions.

Laser-Induced Breakdown Spectroscopy (LIBS)

The technique chosen to measure boron was laser-induced breakdown spectroscopy (LIBS) or laser spark spectroscopy, which had been successfully applied in an earlier project, to measure sodium in flue gas at the Gallo Glass Co. plant in Modesto, California (Buckley, et al., 2000; Walsh and Moore, 2000). In LIBS, a pulsed neodymium-doped yttrium aluminum garnet (Nd:YAG) laser is focused in the gas/droplet/particle mixture to be analyzed. The high electric field at the focal point breaks down the gas and generates a high temperature plasma spark, which vaporizes particles and droplets, dissociates molecules into atoms, and electronically excites and ionizes the atoms. The light emitted as the electrons and ions recombine and return toward their ground states is collected and resolved according to wavelength using a grating spectrometer. The wavelengths of the peaks in the spectrum identify the elements present and, by calibration in the laboratory using aerosols of known composition, the

intensities of the lines can be used to determine the concentrations of individual elements. A schematic diagram of the instrument is shown in Figure 1.

In general LIBS works best for metallic elements, whose atomic emission lines tend to be more intense than those of non-metals such as oxygen, chlorine, and sulfur. The LIBS technique has a number of advantages over traditional extractive sampling methods for determining metals: (1) the measurement is done in-situ, without having to extract a sample of the gas/particle mixture or handling of the particles, (2) the laser fires 9 times per second, so the time resolution of the measurement is excellent, even when large numbers of "shots" are averaged to improve the signal to noise ratio, and (3) typical detection limits for metallic elements in particulate matter are quite low, on the order of 0.1 $\mu g/m^3$, the actual value depending upon the element and its mode of occurrence (whether particulate or vapor and, if particulate, the size and number concentration of the particles).

Electron Micrograph of the Precipitator Dust

Shortly after a planning meeting in July 2000 at the plant in Chowchilla, Mark Stahl sent a sample of dust from the electrostatic precipitator to Sandia for analysis. A semi-quantitative elemental analysis of the dust is given in Appendix A. A scanning electron micrograph of the sample, in Figure 2, shows agglomerates of very fine particles, in which the primary particles have sizes of order 0.1 μm, mixed with nearly spherical particles having sizes as large as 10 μm. In many types of particle samples an energy-dispersive X-ray analysis of individual particles provides valuable information on the variation of particle composition; however, the method does not work well for elements having low atomic weights, such as boron. The elements that could be detected were, beginning with the most abundant: oxygen, sodium, sulfur, potassium, silicon, and calcium. Aluminum and chlorine were observed in some particles. The very fine, 0.1 μm, particles are those produced by condensation of vapor. The source of the large particles is unknown, but possible sources are batch dust, droplets or particles ejected from the surface of batch piles during decomposition, and entrainment of slag from the wall of the vertical flue. Some of the large spherical particles are evidently hollow, as shown by broken shells that could be seen in some of the electron micrographs, though no such particles are visible in Figure 2.

Field Work

The metallic elements present at highest concentration in the sample of dust taken from the electrostatic precipitator prior to the tests were sodium and boron (Appendix A). The specific objective of the field tests was to determine the mass flow rates of these metals as functions of the oxygen to natural gas ratio at the burners. Measurements were made both in the horizontal flue downstream from the furnace and at the exit from the electrostatic precipitator, in order to separate effects of burner adjustment on volatilization and carryover from its effects on precipitator performance. The volumetric flow rate of flue gas at the LIBS measurement points was estimated from measurements of gas velocity at the center of the duct at each location using a Pitot/static probe, so mass

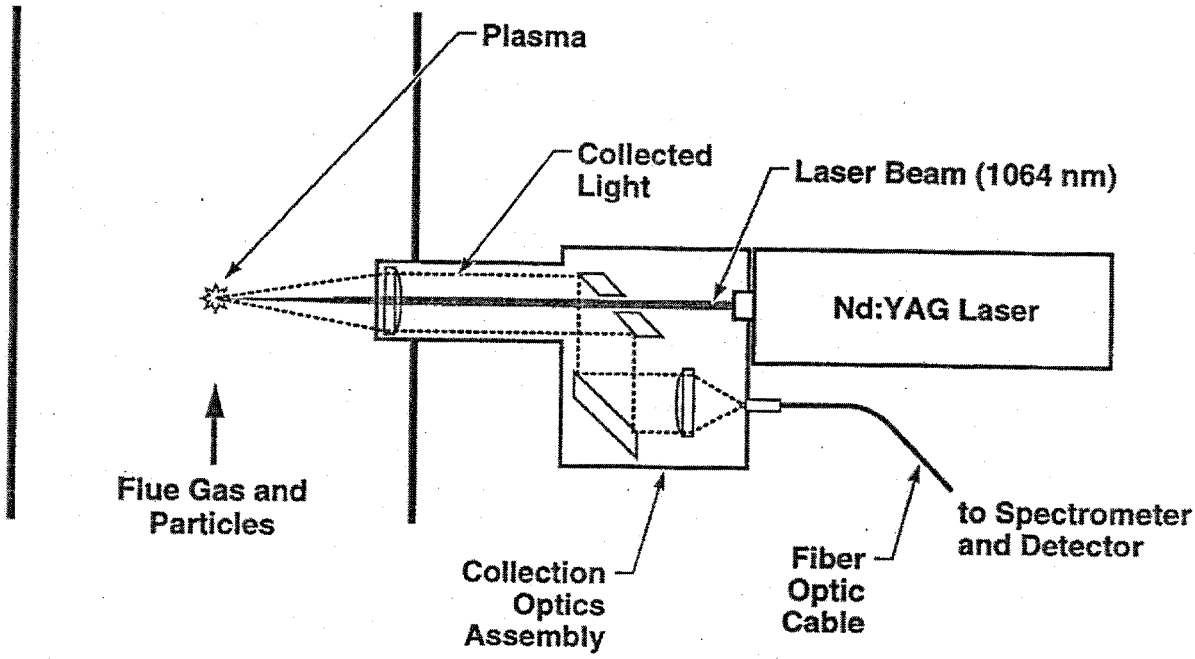

Figure 1. Schematic diagram of the Sandia laser-induced breakdown spectroscopy (LIBS) instrument, showing the arrangement of the optical system for focusing the laser pulses and collecting the light emitted by the spark.

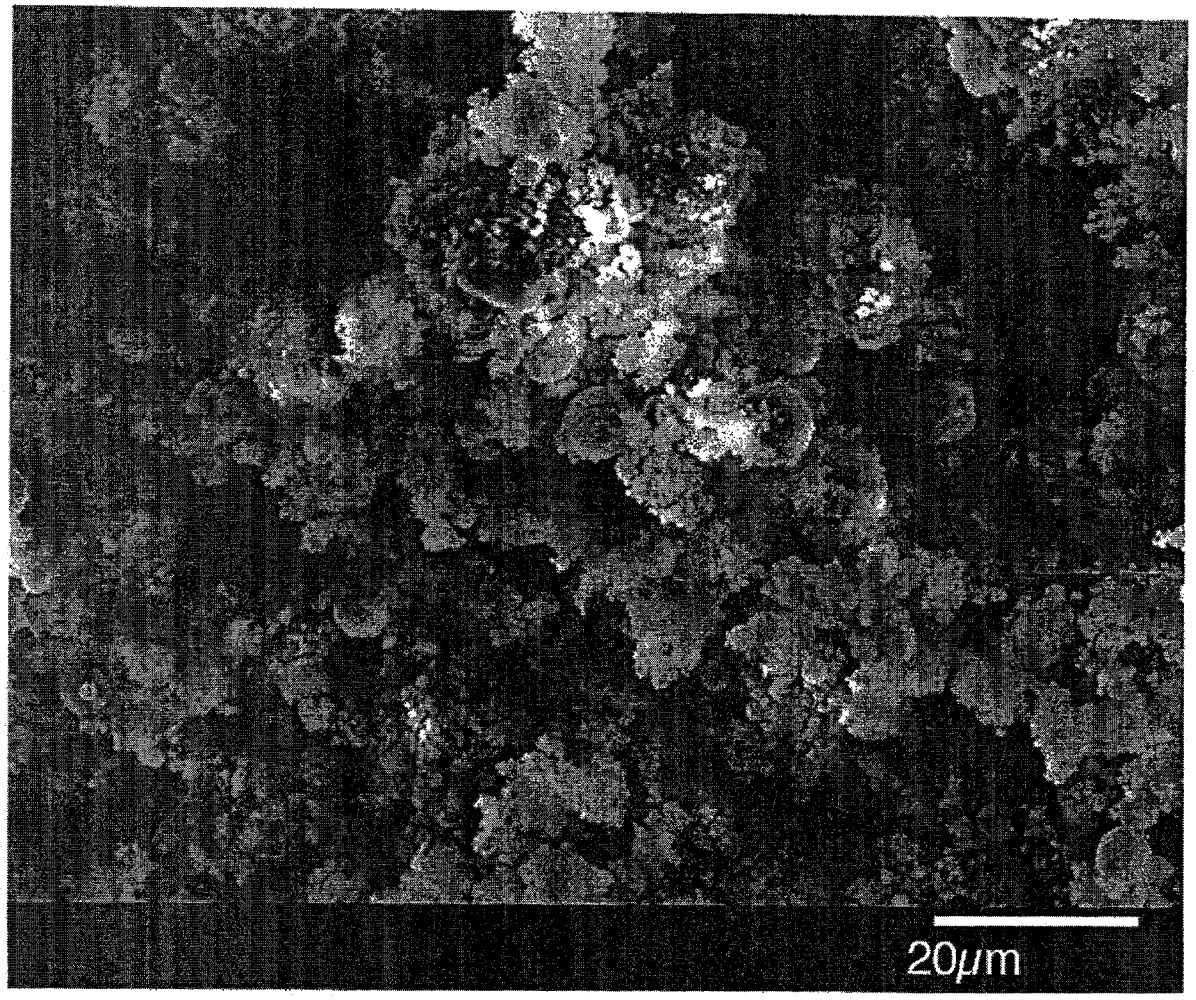

Figure 2. Scanning electron micrograph of particles in a dust sample from the electrostatic precipitator collected by Mark Stahl on July 18, 2000. The micrograph was taken by Jeff Chames in the Analytical Materials Science Department at Sandia National Laboratories.

flow rates of the elements could be determined from the concentration data provided by LIBS. Numerous temperature, pressure, flow rate, and composition data were also recorded to provide information needed to interpret the results.

EXPERIMENTAL MEASUREMENTS AND DATA ANALYSIS

Test Site and Instrumentation

The experiments were done at the CertainTeed Corporation's fiberglass insulation plant in Chowchilla, California. The measurement points were (1) in the horizontal flue downstream from the melting furnace, between the vertical flue at the exit of the furnace and the caustic spray tower, and (2) downstream from the electrostatic precipitator, between the precipitator and the induced draft fan. A photograph of the LIBS instrument mounted on the duct downstream from the electrostatic precipitator is shown in Figure 3. A larger view from a different direction, but at the same location, in Figure 4, shows the geometry of the duct in the vicinity of the measurement point and the instrument rack containing the laser power supply and spectrometer. This rack must be within 8 feet or so of the laser and optical system in order that the information carried by the light from the laser spark not be degraded in its transmission by optical fiber from the instrument package mounted on the duct to the spectrometer.

Adaptation of LIBS to the Problem

There is only one boron emission line, at 249.7 nm, in the region of the spectrum accessible to the LIBS instrument (220 to 900 nm). This peak is close to a strong emission line of carbon, which is always present at high concentration in the products of fossil fuel combustion. There was concern about whether or not the boron and carbon peaks could be resolved well enough to obtain high quality data for boron. As a result of preliminary work in the laboratory prior to the tests and fine tuning at the site, excellent separation of the peaks was achieved, as shown in Figure 5, by adjusting the time delay following creation of the spark before beginning to collect the emitted light, and by adjusting the duration of the interval over which the signal was integrated. Some sacrifice of the boron signal intensity was required, but not enough to compromise the quality of the data. Silicon also emits at several wavelengths slightly longer than the wavelength of the boron peak, as also shown in Figure 5, but the silicon concentration was not high enough for these peaks to interfere with the determination of the area under the boron peak.

The LIBS signal intensities from boron in the horizontal flue indicated that the boron concentrations there were much higher than could be run in the laboratory calibration apparatus. Because the calibration relating concentration to intensity cannot be assumed to be linear at high concentrations, only relative values of boron concentration could be determined at that location. The boron concentrations at the electrostatic precipitator outlet were within the range covered in the calibration procedure.

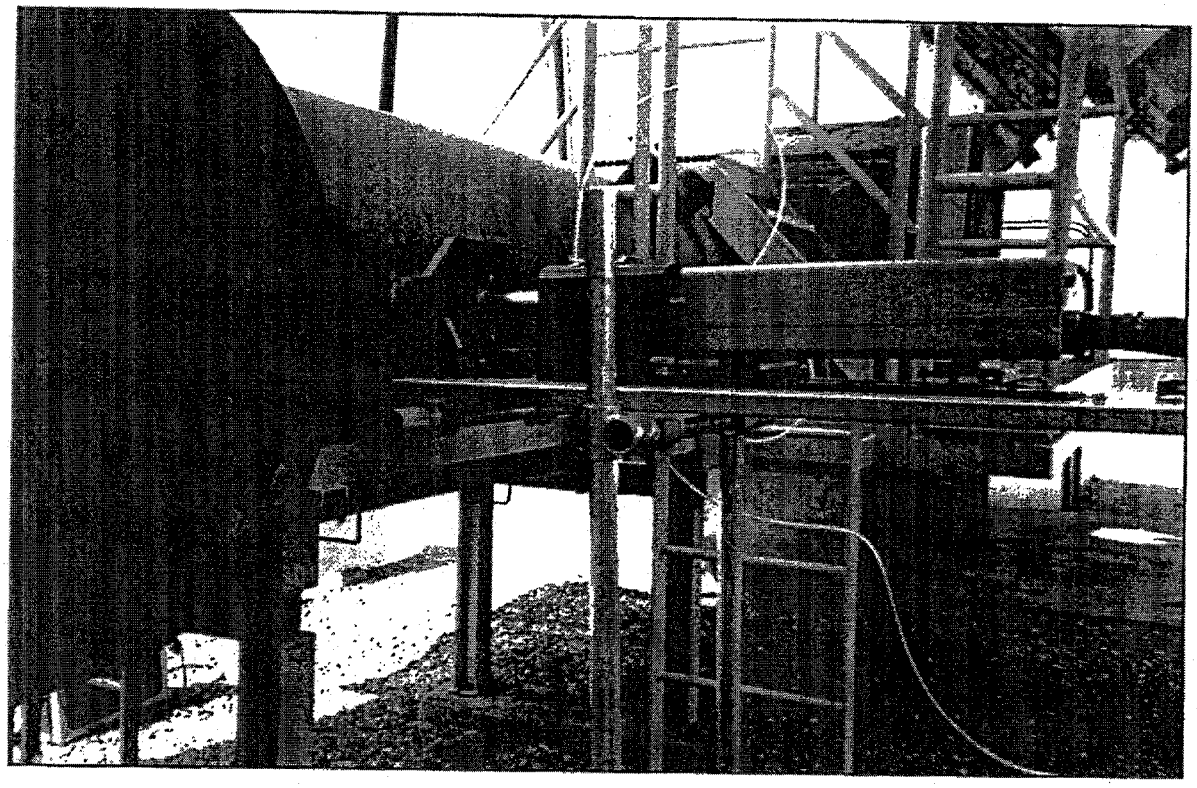

Figure 3. Close-up photograph of the LIBS instrument mounted on the duct downstream from the electrostatic precipitator. The orientation of the figure and the equipment pictured are approximately the same as in the diagram of Figure 1.

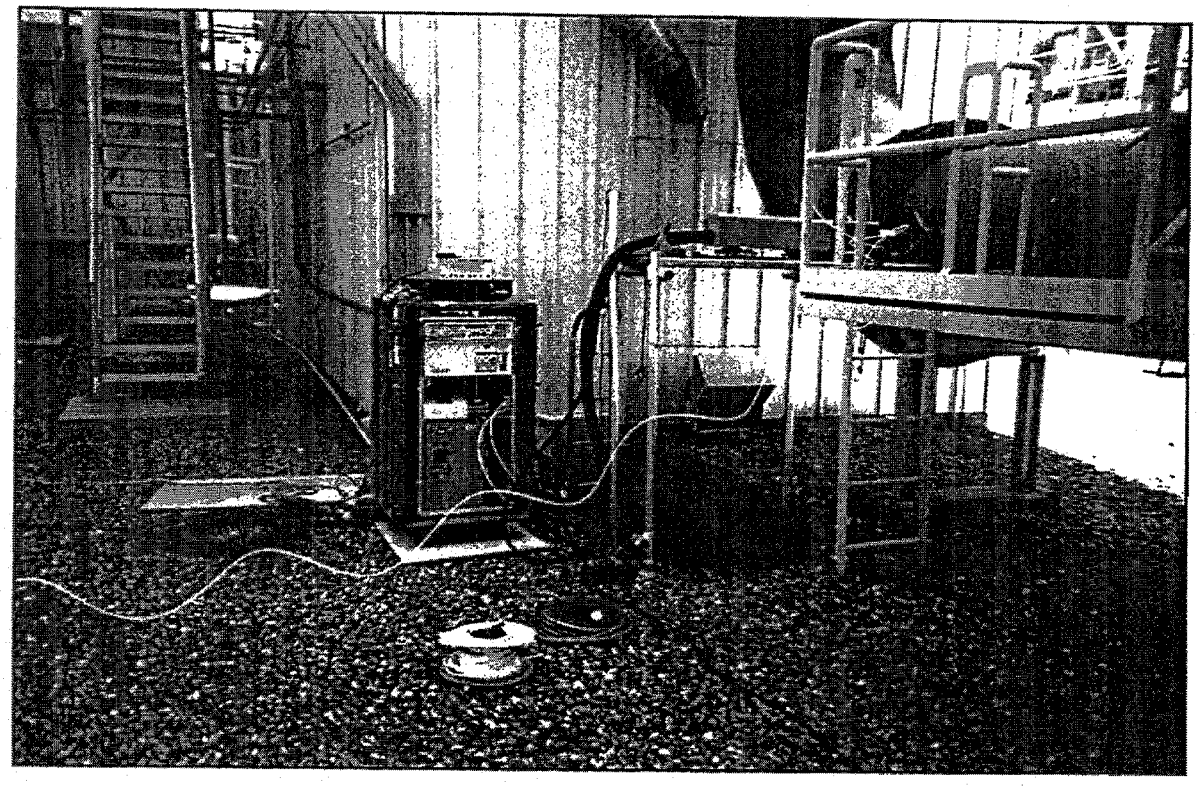

Figure 4. View from the direction opposite to that in Figure 3, of the LIBS equipment at the sampling location downstream from the electrostatic precipitator. The instrument package on the ground to the left contains the laser power supply, the spectrometer, and the CCD camera used to record the spectrum of the light emitted by the laser spark.

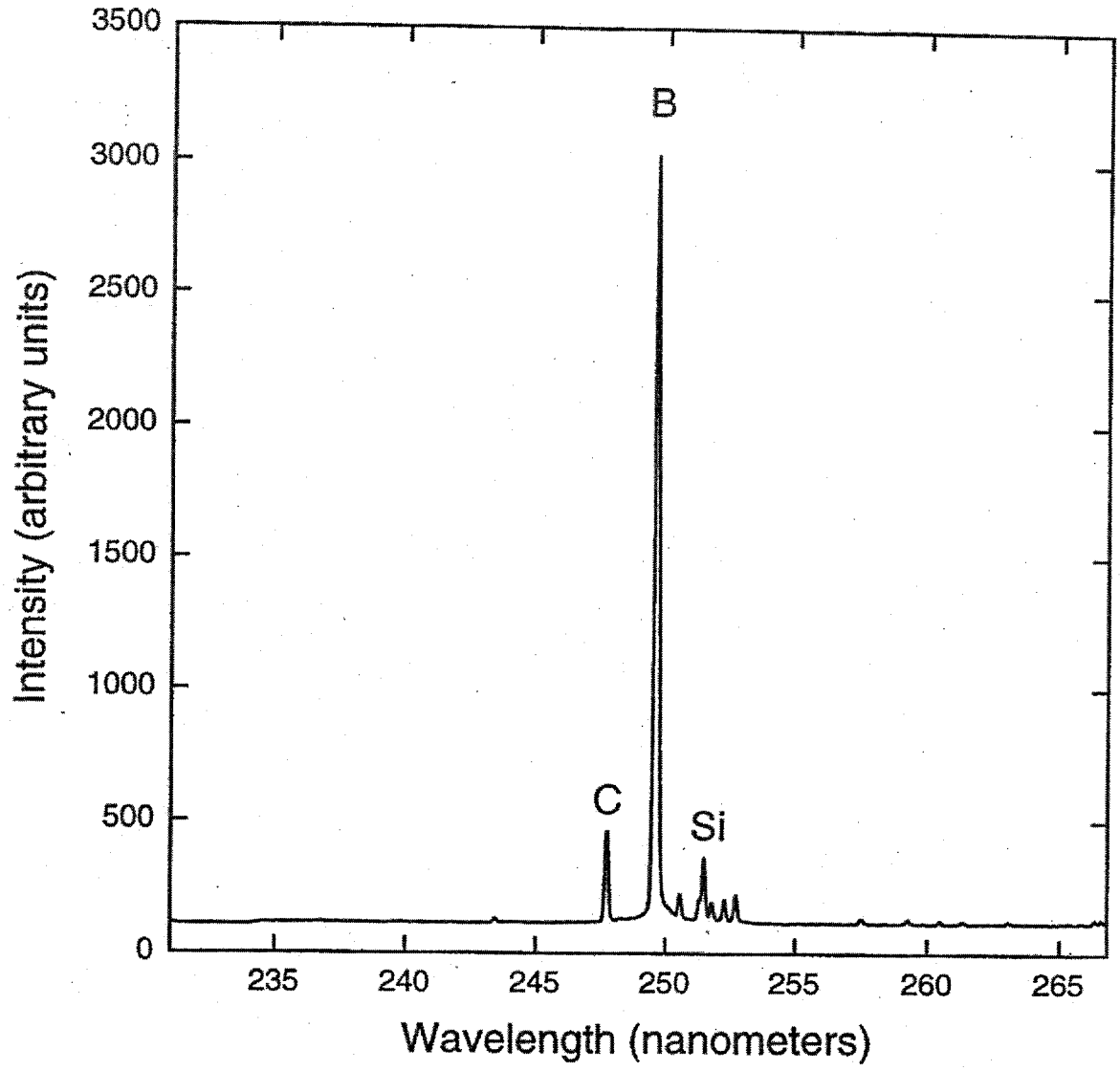

Figure 5. Typical spectrum obtained by superimposing the individual spectra generated by 1000 laser sparks in the horizontal flue, showing good separation of the boron peak from the carbon and silicon peaks.

The most intense emission line of sodium, at 589.0 nm, is normally used to measure sodium using LIBS; however, the concentration of sodium in the horizontal flue was so high that the emission from this line (and also from a slightly weaker line adjacent to it) was self-absorbed, i.e. emission from sodium in the hottest portion of the spark was adsorbed by cooler sodium atoms at the spark boundary. In the presence of self-absorption, the area under an emission peak no longer has a well-defined relationship to concentration, invalidating the calibration procedure. Other sodium peaks were examined during the initial work at the test site and the emission line at 568.2 nm, associated with an electronic transition between higher-lying energy levels and therefore less likely to be self-absorbed, was chosen for the measurements. Emission from the 568.2 nm line was well-behaved under the conditions of sodium concentration in the horizontal flue, but, as in the case of boron, the concentrations of sodium were higher than could be run in the calibration rig in the laboratory, so only relative sodium concentrations could be obtained at that location. In contrast, the sodium levels at the precipitator outlet were low, so the usual 589.0 nm emission line was used for the sodium measurements at that location.

Test Program and Procedure

The Sandia team left Livermore on Monday morning, August 28, 2000 and, with the help of many people from CertainTeed, began the set up of the equipment on the horizontal flue the same day. The following day was devoted to preliminary measurements and optimization of the LIBS instrument settings, including the adjustments described above. The measurements in the horizontal flue (7 runs) were made on August 30 and the equipment moved to the duct downstream from the electrostatic precipitator. Measurements at the exit from the electrostatic precipitator (10 runs) were made on August 31. The LIBS equipment was packed up and taken back to Livermore on Friday. One member of the Sandia group stayed behind to record the spectrum of light emitted from the combustion space on Friday and Saturday, September 1 and 2.

The procedure for a run was to set the oxygen to gas ratio at a desired value, then wait until the NO_X reading in the stack became steady, usually 20 to 30 minutes. Typically six, sometimes more, sets of LIBS data were collected in the range of wavelengths containing the boron peak, each set consisting of the average of the emission from 1000 sparks. The grating in the spectrometer was then changed to the range containing the peak for sodium, and six 1000-shot averages again recorded. The grating was then returned to the range containing the boron peak and, when time permitted, more data (usually another six sets) were recorded for boron. In the latter cases, all at the precipitator outlet, there are two separate sets of measurements for boron at the same test condition. The oxygen to gas ratio was then changed to a new value, and the process repeated. A minimum of three people were required: one from CertainTeed to set the furnace conditions, one from Sandia to collect the LIBS data, and another from Sandia to measure the gas velocity and record the process data. The conditions during the runs are given in Table 1.

Table 1.
Conditions during the Measurements of Boron and Sodium in the Horizontal Flue and at the Electrostatic Precipitator Outlet.

Run No.	Date, 2000	Sampling Location	--- Clock Time --- start	end	Ambient Temp., °F	Barometric P, mm Hg	Relative Hum., %	O_2/n.g. v/v	O_2 Purity, %	- Flows, kscfh - O_2	n.g.
1	8/30	flue	9:27 am	10:07	76.0	(753.3)	60.5	1.85	93.30	109	47.85
2	8/30	flue	10:37	11:06	77.7	753.3	56	2.0	92.93	117.6	47.9
3	8/30	flue	---	12:06 pm	73.0	753.3	70	1.9	92.63	109.85	47.7
4	8/30	flue	1:18 pm	1:40	73.4	753	69	1.8	92.96	99.53	45.7
5	8/30	flue	2:03	2:38	74.2	752	70	1.7	93.20	96.18	45.7
6	8/30	flue	3:09	3:41	73.5	752	73	1.6	93.35	87.0	43.65
7	8/30	flue	4:17	4:49	74.8	751.35	69	1.85	92.08	106.58	45.83
8	8/31	EP outlet	10:40 am	11:53	77.3	756.0	70.5	1.85	92.46	105.25	46.1
9*	8/31	EP outlet	12:23 pm*	---	82.4	755.2	62	2.0	(92.39)	(118)	(48)
10*	8/31	EP outlet	12:49	2:08	(89)	(754.5)	(55.5)	1.95	92.32	115.13	47.85
11	8/31	EP outlet	---	3:50	96.0	(753.8)	49	1.7	99.73	86.07	43.55
12	8/31	EP outlet	4:10	4:49	96.0	753.8	49.5	1.6	92.43	88.73	43.93
13	8/31	EP outlet	5:22	5:52	88.9	753.8	57	1.75	91.49	101.25	46.73
14	8/31	EP outlet	6:29	7:12	79.0	753.8	65	1.65	91.70	91.74	44.88
15	8/31	EP outlet	7:52	8:31	72.9	754.0	75	1.7	91.42	96.55	45.89
16	8/31	EP outlet	9:40	10:29	69.5	754.5	80	1.95	92.62	117.85	48.35
17	8/31	EP outlet	10:59	11:36	69.2	754.5	80.5	1.85	92.19	107.26	46.45

Notes are at the end of the table.

Table 1 (continued)

Run No.	------- Furnace ------- P, in.w.c.	Temp., °F	Water Flow, gpm	Gas Temp. °F	Static P, Pa	Pitot/Static ΔP, Pa	EP Temp., °F in	out	--- Opacity, % --- 1 min.	3 min.	NOx lb/hour
1	0.006	2378	5.75	809	-420	322.5	586	454	0.06-0.20	---	39.4
2	0.008	2381	6.01	808	-449	337.5	591	455	0.36	---	52.1
3	0.008	2378	5.8	810	-430	325	590	455	0.37	---	49.6
4	0.008	2378	5.3	808	-370	295	582	453	0.23	0.20	39.1
5	0.008	2379	5.25	809	-335	285	580	450	0.53	0.50	29.1
6	0.008	2377	5.1	808	-282.5	255	575	448	0.89	0.70	14.3
7	0.008	2377	5.7	808	-415	315	586	451	0.29	0.40	41.0
8	0.006	2377	5.5	412	-1862	16.5	574	444	0.38	0.30	37.7
9*	---	---	(6)	(420)	-2358	(20)	---	---	---	---	---
10*	0.005	2378	6.1	420	-2234	20	592	459	0.21	0.20	46.5
11	0.005	2382-2377	4.87	425	-1737	14	581-585	459	0.54-0.63	0.70	21.5-28.8
12	0.005	2376	5.1	424	-1489	14	580	457	0.57-1.17	0.50	19.5
13	0.005	2378	5.6	421	-1862	16	585	457	0.49	0.50	31.8
14	0.005	2381	5.15	419	-1737	14.25	580	455	0.86	0.90	20.8
15	0.005	2377	5.2	414	-1737	14	575	452	0	0.30	23.4
16	0.005	2378	6.3	418	-2110	18	583	453	0.07	0.10	48.0
17	0.005	2378	5.7	417	-1986	16.5	583	455	0.30	0.40	42.3-46.1

*Camera pulled out at 12:23 pm until the end of Run No. 10.
( ) Estimated by interpolation or extrapolation of other measurements.
--- Measurement not available.

Determination of Gas Flow Rate

The area under the emission peak for an element is proportional to the mass of the element in the laser spark and, since the spark volume is fixed, proportional to the concentration (mass or number of atoms per unit volume) of the element in the gas/particle mixture. The proportionality constant is determined by measuring, in the laboratory, the LIBS signals from sprays of aqueous solutions of a salt of the metal at several concentrations covering the range of interest. However, the quantity of greatest interest from the point of view of emissions is not the concentration of an element, but its mass flow rate, which is equal to the product of its concentration and the volumetric flow rate of gas.

The volumetric flow rate at each measurement point and run condition was estimated from measurements of the difference between the static and dynamic pressures of the gas on the centerline of the duct, using a Pitot/static probe (United Sensor Corp., Amherst, NH) and inclined manometer. The Pitot/static pressure difference is given by

$$\Delta P = \frac{1}{2}\rho u^2 \qquad (1)$$

where ρ is the density of the gas and u is its velocity. The average gas velocity over the cross section of each duct was estimated using a correlation derived from the Reynolds number dependence of the ratio of average velocity to maximum velocity for fully-developed flow in circular ducts (Green and Maloney, 1984). This is expected to have been a good approximation in the horizontal flue, where there were long runs of straight pipe upstream and downstream from the measurement point, but it may not have been such a good approximation at the outlet from the electrostatic precipitator, where there was an 90° elbow a short distance upstream from the measurement location and a transition downstream to a larger, square cross section at the entrance to the induced draft fan, as shown in Figures 4 and 3, respectively.

Determination of the gas density, for calculation of the velocity using Equation (1), requires knowledge of its absolute static pressure and temperature, both of which were measured, and its average molecular weight, which depends upon the gas composition. Evaluation of the Reynolds number requires the gas density and, in addition, the viscosity, which also depends upon composition. Determination of the composition of the gas is complicated by the fact that an unknown quantity of air leaks into the ductwork downstream from the location in the flue at which the gas pressure drops below atmospheric. The melting furnace was at slightly positive pressure, but at the electrostatic precipitator outlet, just upstream from the induced draft fan, the pressure was approximately – 8 in. w. c. (Table 1).

The gas composition and total flow rate were estimated using the following procedure. First, an initial, low, guess was made of the air inleakage, then the volumetric flow rate of gas at the actual conditions of temperature and pressure in the duct were determined from the air, natural gas, oxygen, batch oil, and batch gas flow rates and

compositions, plus the steam derived from quench water and caustic soda solution. Analyses of the natural gas and batch oil are given in Appendix B. The composition of the air included nitrogen, oxygen, water vapor (the humidity of the ambient air was measured during each run, the values are given in Table 1), carbon dioxide, and argon. The composition of the resulting flue gas mixture was then used to calculate its density and viscosity, and these were used, along with the flow rate, to evaluate the Reynolds number and calculate a new value for the volumetric flow rate from the Pitot/static pressure difference on the centerline. If the two flow rates were not in agreement, the initial estimate of the air inleakage was increased by a small amount and the calculation repeated until the volumetric flow rates from the feeds and from the Pitot/static ΔP agreed to within negligible error. The increments in air flow rate were made small enough that iteration was not necessary. The computer code used for the calculations is attached as Appendix C. Viscosities of the gas mixtures were evaluated using the method described by Golubev (1970), including contributions from nitrogen, oxygen, steam, carbon dioxide, and argon.

The values for the gas flow rates in the horizontal flue and at the precipitator outlet, calculated as described above, are shown as functions of the oxygen to gas ratio in Figure 6. The numerical values are given in Tables 2, 3, 4, and 5, where they are used for the calculation of boron and sodium flow rates from the LIBS concentration measurements. Comparison of the flow rates at a common temperature and pressure shows that the flow rate at the precipitator outlet was typically 20% larger than the flow rate in the horizontal flue, due to the contributions of steam from the caustic soda solution and additional air entering the flow downstream from the horizontal flue.

NO_X Emission

The NO_X emission reading from the stack gas monitor, displayed in the control room, was recorded at each run condition. The values are given in the last column of Table 1 and their dependence on the oxygen to natural gas ratio is shown in Figure 7.

Spectrum of Light Emitted by Gaseous Species in the Combustion Space

After completion of the boron and sodium measurements, a completely separate set of observations was made of the spectrum of light emitted from the combustion space. The objective of this work was to see if emission from BO_2 could be used to map out an approximate spatial distribution of boron in the combustion space and identify regions where it is preferentially volatilized and highly concentrated, as had been done for sodium in a Gallo Glass Co. furnace (Buckley et al., 2000; Walsh and Moore, 2000). The emission spectrum was obtained by collecting light emerging through the peep hole at the base of the vertical flue, sighting along the entire length of the furnace. The spectrum contained strong emission from sodium and potassium atoms, weaker emission from rubidium and lithium atoms, and a very weak emission, possibly from BO_2, in the vicinity of 547 nm. Attempts to increase the intensity of this signal by looking along higher temperature paths, through the flames, were not successful. It was concluded that no emission that could serve as the basis for a useful diagnostic technique for boron was

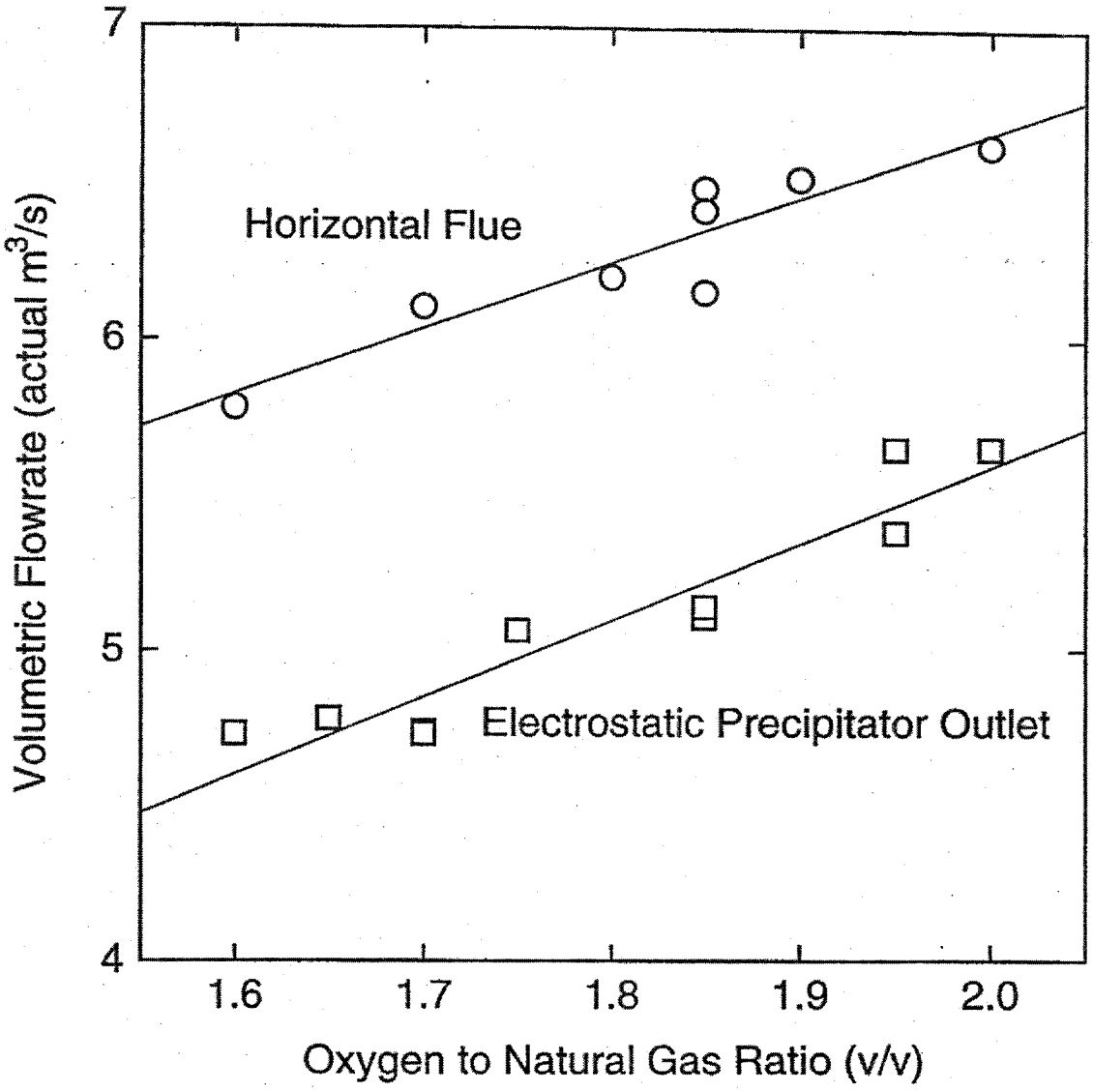

Figure 6. Volumetric flow rates of gas in the horizontal flue and at the electrostatic precipitator outlet as functions of the oxygen to natural gas ratio. The volumes are specified at the actual conditions of temperature and pressure in the ducts. The pressures have little effect on the flow rates, but the temperatures at the two locations are quite different, approximately 809 °F in the horizontal flue and 419 °F at the electrostatic precipitator outlet (the values for each run condition are given in Table 1). Reduction of the two flow rates to common temperature and pressure shows that the flow rate at the precipitator outlet is typically 20% larger than that in the horizontal flue, due to the water and air introduced in the caustic spray tower and inleakage of air.

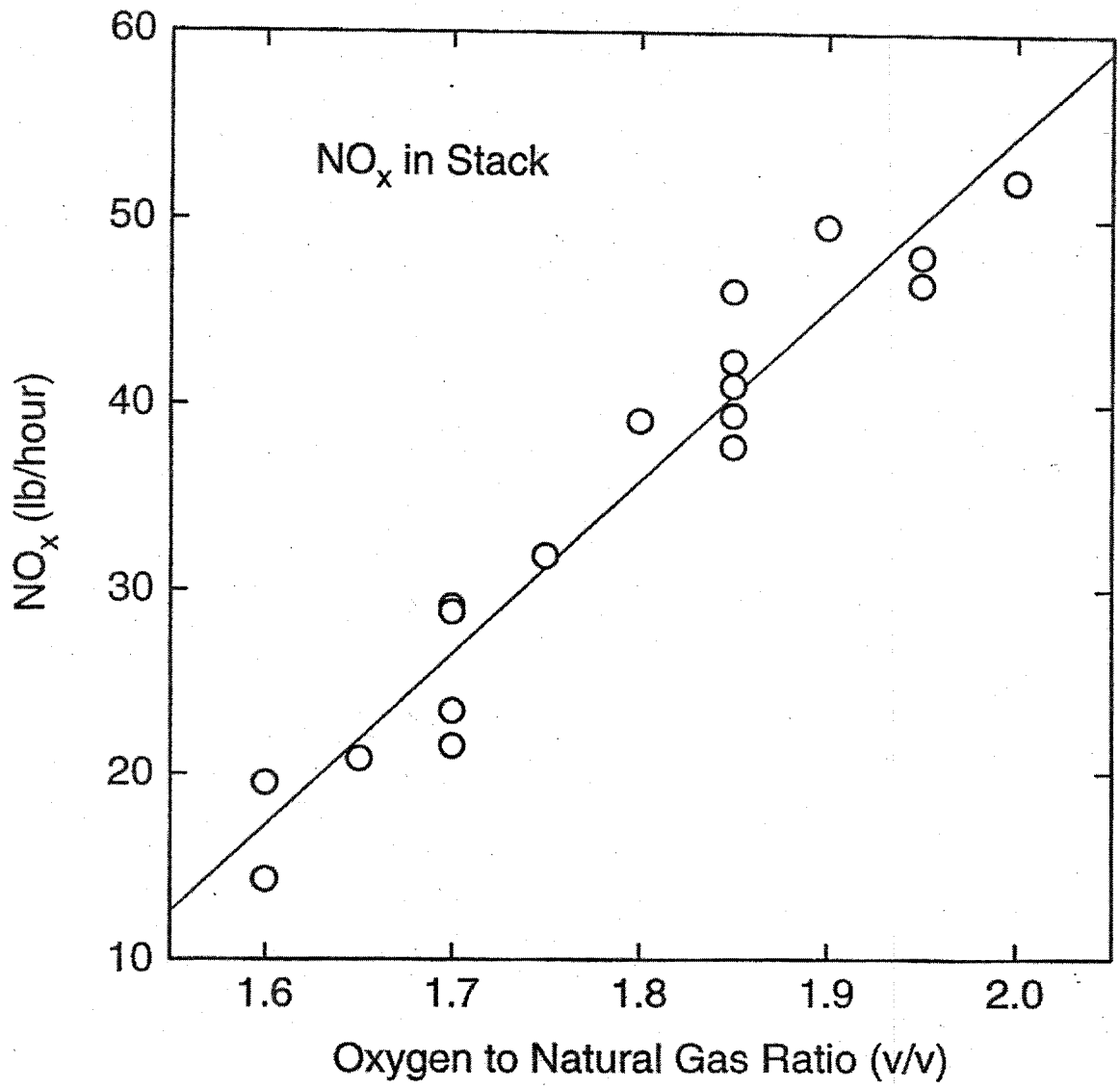

Figure 7. Nitrogen oxides in the stack gas as a function of the oxygen to natural gas ratio.

present in the wavelength range of the spectrometer, from 300 to 900 nm. Laser-induced fluorescence, or other more exotic methods, might be possible, but these should first be investigated at smaller scale in the laboratory.

RESULTS AND DISCUSSION

Boron

As mentioned above, absolute concentrations of boron in the horizontal flue could not be derived, with any certainty, from the LIBS measurements because the concentrations indicated by the boron LIBS signal intensities were 7 to 8 times higher than the highest concentrations of boron that could be run in the laboratory calibration rig. Relative average concentrations of boron, from the relative intensities of the LIBS signals from boron in the horizontal flue, are given in third column of Table 2. The standard deviation of the six or more 1000-shot averages is given in the column to the right of the average. The gas flow rates, determined by the procedure outlined in the previous section, are in the fifth column. The relative mass flow rates of boron, equal to the products of its concentration and the gas flow rate, are given in the next-to-last column, followed by the standard deviation of the measurements.

The calculation of the mass flow rate of boron from its concentration is illustrated by the plots shown in Figure 8. The boron concentration is at the top, in Figure 8a, and the corresponding values of the gas flow rate are shown in Figure 8b. The mass flow rate, equal to the product of the boron concentration and gas flow rate, is shown in Figure 8c. The mass flow rate of boron in the horizontal flue is practically independent of the oxygen to gas ratio, suggesting that the flux (mass or moles per unit area per unit time) of boron-containing species from the surface of the molten glass in the furnace is not sensitive to burner adjustment. The decrease in boron concentration with increasing oxygen to gas ratio, shown in Figure 8a, is then the result of increasing dilution of an approximately constant rate of boron loss by an increasing volume of combustion products. The results for the mass flow rate of boron, from Figure 8c, are shown in a larger format in Figure 9. In these figures and the others which follow, error bars indicate the standard deviations of the results from the six or more 1000-shot averages, with the exception of Figure 12, where the range of the measurements at each oxygen to gas ratio is shown instead.

The measurements of boron concentration and mass flow rate at the outlet from the electrostatic precipitator are given in Table 3. The concentrations and flow rates are those of elemental boron, not a hypothetical boron compound. If one wished, for example, to assume that all of the boron were present as metaboric acid, its mass flow rate would be estimated by multiplying the boron mass flow rate by the ratio of the molecular weight of HBO_2 to the atomic weight of boron, 43.82/10.811 = 4.1. In contrast to the approximately constant flow rate of boron in the horizontal flue, the flow rate at the precipitator outlet shows a marked dependence on the oxygen to gas ratio, as shown in Figure 10. The boron flow rate decreases by roughly 30% on going from an oxygen to

Table 2.
Relative Concentrations and Mass Flow Rates of Boron in the Horizontal Flue.

Run No.	O_2/n.g. v/v	-B Conc., arb. units- ave.	std. dev.	Gas Flow actual m^3/s	-B Flow, arb. units- ave.	std. dev.
1	1.85	14.01	0.53	6.488	90.9	3.4
2	2.0	13.11	0.28	6.629	86.9	1.9
3	1.9	13.68	0.43	6.521	89.2	2.8
4	1.8	13.41	0.40	6.201	83.2	2.5
5	1.7	13.74	0.51	6.105	83.9	3.1
6	1.6	15.69	0.46	5.780	90.7	2.7
7	1.85	12.95	0.20	6.417	83.1	1.3

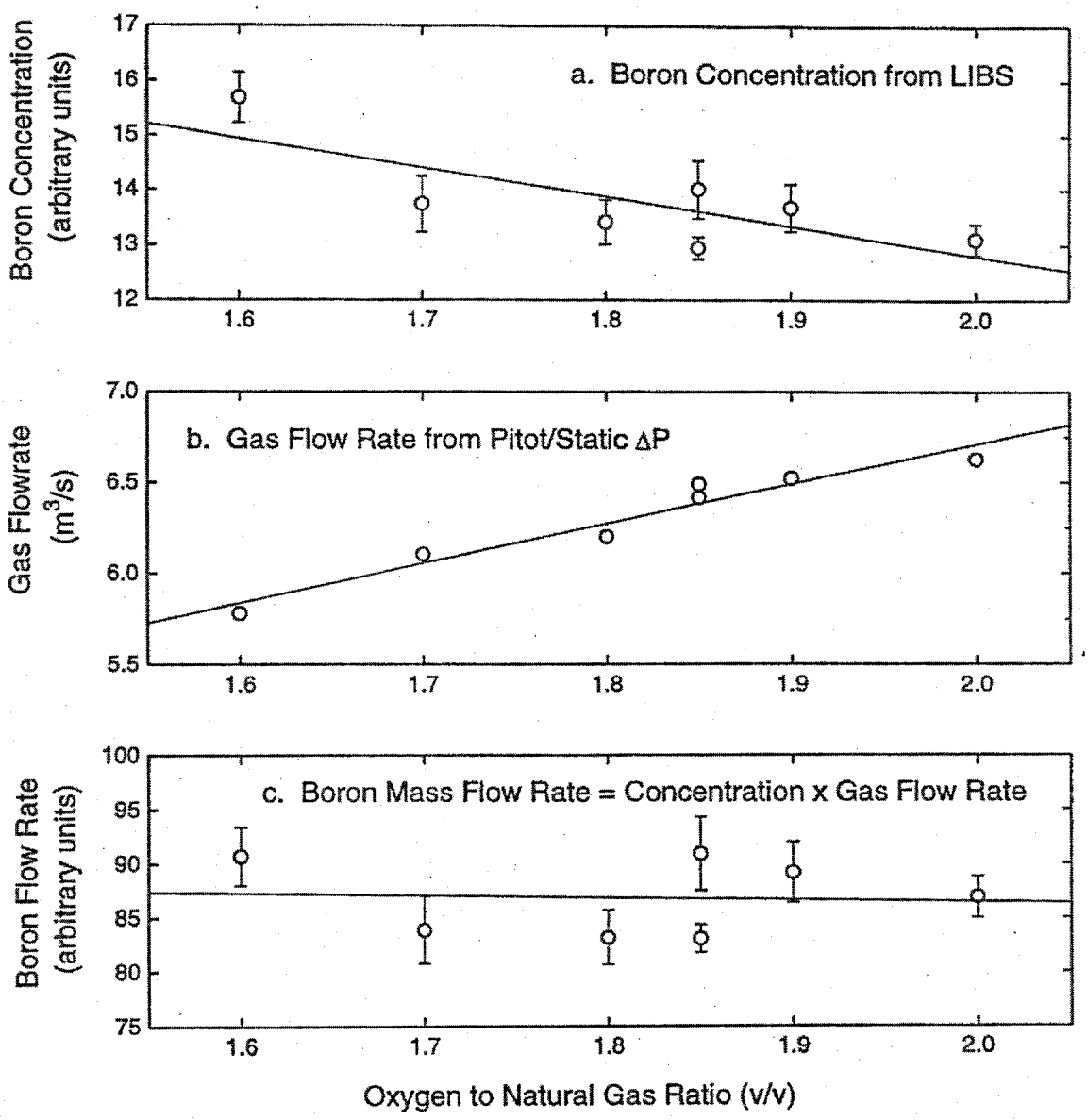

Figure 8. Example showing the dependence of: a. the boron concentration in flue gas, b. the volumetric flow rate of flue gas, and c. the mass flow rate of boron, on the oxygen to natural gas ratio. The decrease in concentration with increasing oxygen to gas ratio is due almost entirely to dilution by the increasing gas flow, so the boron mass flow rate, equal to the product of its concentration and the gas flow rate, is nearly constant.

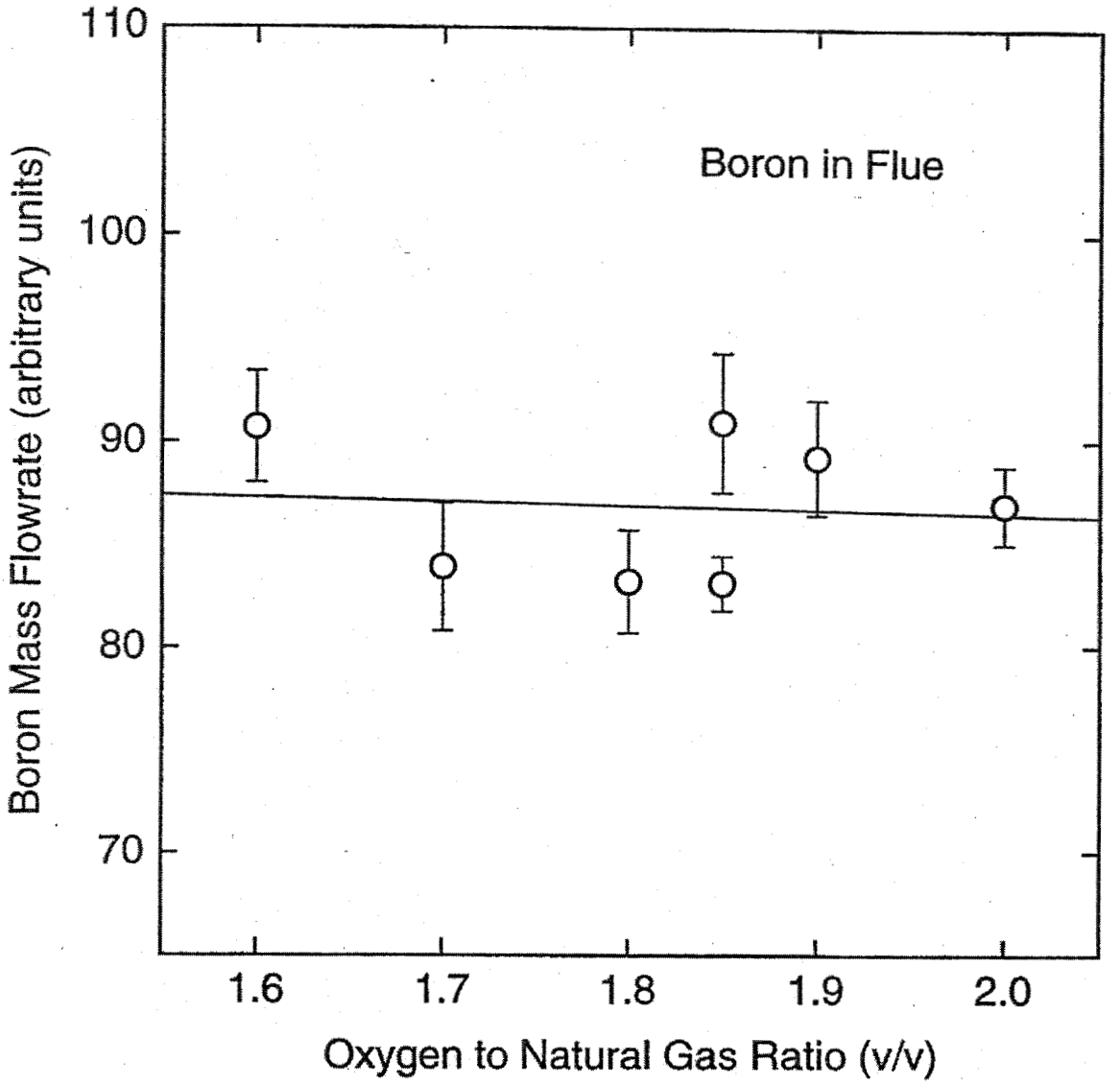

Figure 9. Dependence of boron mass flow rate in the horizontal flue on oxygen to natural gas ratio. (Same data as shown in Figure 8c.) Relative, rather than absolute, mass flow rates are given because the boron concentration was outside the range that could be run in the laboratory calibration apparatus.

Table 3.
Concentrations and Mass Flow Rates of Boron at the Electrostatic Precipitator Outlet.

Run No.	O_2/n.g. v/v	- B Conc., mg/m³ - ave.	std. dev.	Gas Flow actual m³/s	- B Flow, lb/hour - ave.	std. dev.
8	1.85	1.530	0.025	5.106	0.0620	0.0010
9	2.0	1.526	0.026	5.652	0.0684	0.0012
10a	1.95	1.623	0.020	5.650	0.0728	0.0009
10b	1.95	1.728	0.053	5.650	0.0775	0.0024
11a	1.7	1.970	0.049	4.737	0.0740	0.0018
11b	1.7	2.219	0.068	4.737	0.0834	0.0025
12a	1.6	2.454	0.051	4.729	0.0921	0.0019
12b	1.6	2.659	0.047	4.729	0.0998	0.0018
13a	1.75	2.103	0.032	5.064	0.0845	0.0013
13b	1.75	2.057	0.023	5.064	0.0827	0.0010
14a	1.65	2.281	0.041	4.778	0.0865	0.0016
14b	1.65	2.231	0.134	4.778	0.0846	0.0051
15	1.7	1.933	0.029	4.729	0.0725	0.0011
16a	1.95	1.596	0.038	5.382	0.0682	0.0016
16b	1.95	1.612	0.049	5.382	0.0689	0.0021
17	1.85	1.677	0.015	5.141	0.0684	0.0006

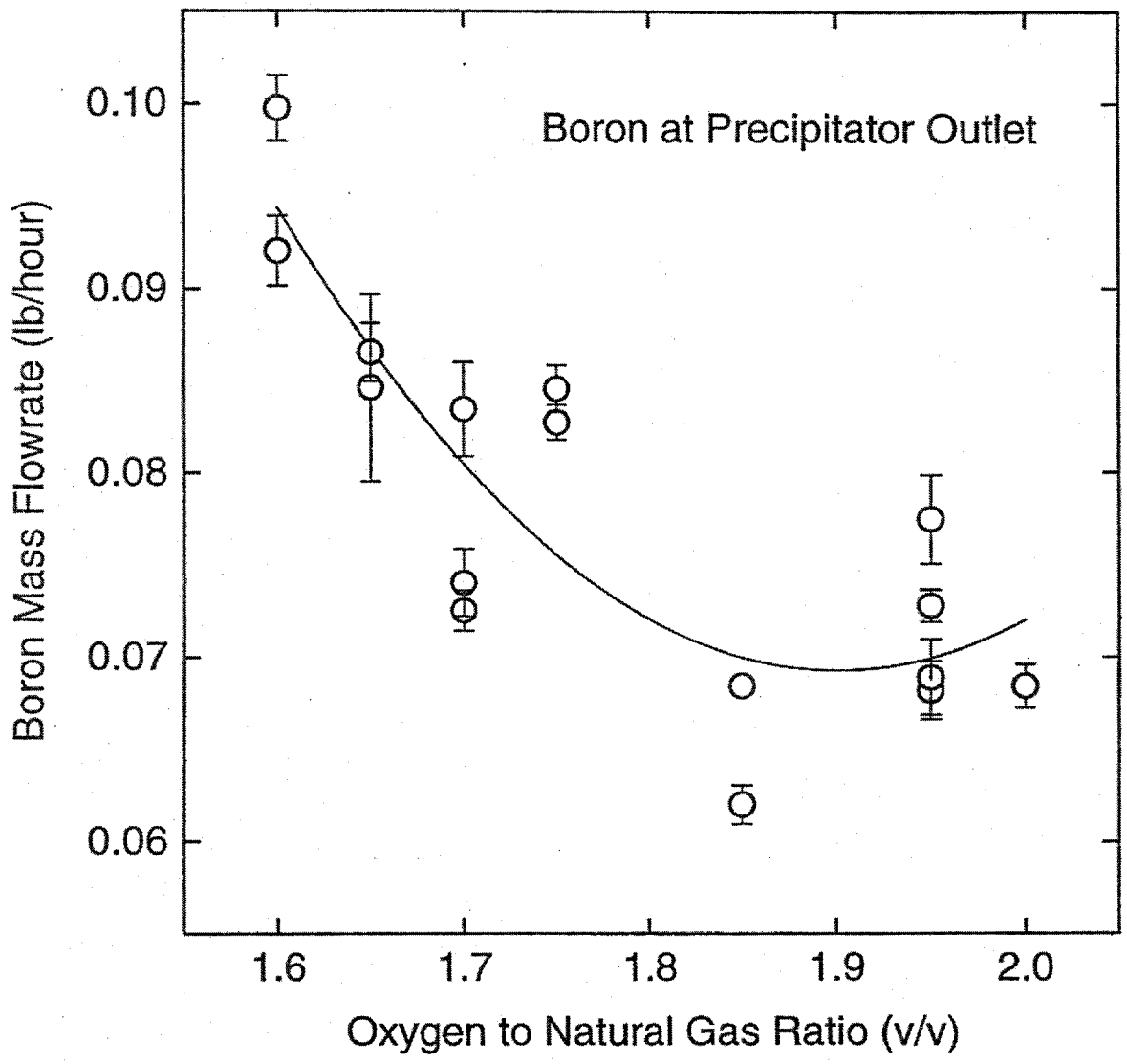

Figure 10. Dependence of boron mass flow rate at the electrostatic precipitator outlet on oxygen to natural gas ratio.

gas ratio of 1.6 to a ratio of 1.85. The curve shown in the figure is a least squares fit of a second-order polynomial to the data, and suggests that the boron mass flow rate begins to increase again at higher oxygen to gas ratios. The upward trend at high oxygen to gas ratio should be viewed as tentative, however, because the scatter of the data is too great to firmly support such a conclusion.

Considering the absence of any significant trend in the flow rate of boron leaving the furnace, shown in Figure 9, inspection of Figure 10 indicates that the efficiency with which boron was removed from the flue gas by the electrostatic precipitator increased as the oxygen to gas ratio was increased from 1.6 to 1.85, then passed through a maximum near an oxygen to gas ratio of 1.85. Considering the trends of NO_X and boron emissions, Figures 7 and 10, respectively, the Chowchilla Plant personnel have done quite a good job of identifying the optimum oxygen to gas ratio at which to operate the furnace.

The authors are not aware of any explanation for the variation in collection efficiency with stoichiometry of the combustion products. Evidently the vapor pressure of some boron species at the temperature in the electrostatic precipitator depends upon the oxygen or carbon monoxide content of the gas. This question warrants further investigation using one of the equilibrium codes developed to calculate the thermodynamic properties of mixtures of inorganic compounds, such as ChemSage, F*A*C*T, HSC, or MTDATA.

Sodium

The sodium concentrations in the horizontal flue were higher than the maximum sodium concentration that could be run in the calibration apparatus in the laboratory, so the LIBS signals from sodium in the flue could not be converted to absolute concentrations. Determination of relative values was, however, possible by comparison of the sodium emission intensities for the various run conditions. The results are given in Table 4 and shown graphically in Figure 11. In contrast to the trend for boron in the flue, sodium increased significantly with increasing oxygen to gas ratio. Evidently, the vapor pressure of sodium species at the surface of the molten borosilicate glass is higher at stoichiometric than under rich combustion conditions. It is difficult to imagine that the increase in sodium volatilization could have been due, say, to an increase in mass transfer from the glass surface to the bulk furnace gas as burner and flame gas velocities increased, because such an effect is expected to be small and because no such trend was observed in the boron measurements.

Sodium flow rates at the precipitator outlet were very low and highly variable, as shown by the results in Table 5 and Figure 12. Sodium emissions were below 0.01 lb/hour in all cases. Because the variability in the sodium mass flow rates was so great, the standard deviations of the measurements have little meaning, so the error bars in Figure 12 show the ranges of the measurements (maximum and minimum values) instead.

Table 4.
Relative Concentrations and Mass Flow Rates of Sodium in the Horizontal Flue.

Run No.	O_2/n.g. v/v	Na Conc., arb. units ave.	std. dev.	Gas Flow actual m^3/s	Na Flow, arb. units ave.	std. dev.
1	1.85	1.0867	0.0148	6.488	7.051	0.096
2	2.0	1.0437	0.0243	6.629	6.919	0.161
3	1.9	1.0265	0.0112	6.521	6.694	0.073
4	1.8	0.9993	0.0082	6.201	6.197	0.051
5	1.7	1.0071	0.0152	6.105	6.148	0.093
6	1.6	0.8737	0.0204	5.780	5.050	0.118
7	1.85	0.9673	0.0107	6.417	6.207	0.069

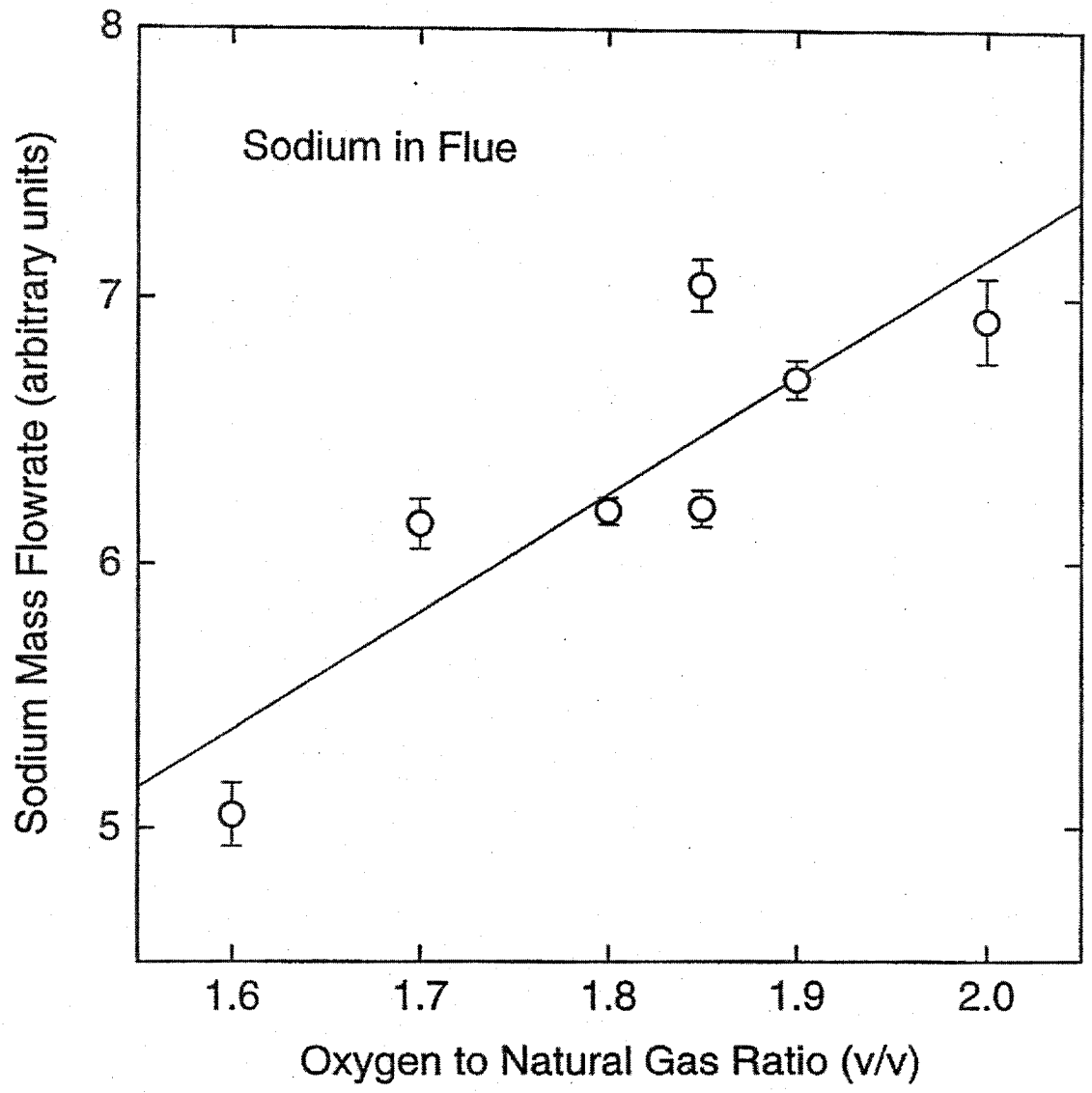

Figure 11. Dependence of sodium mass flow rate in the horizontal flue on oxygen to natural gas ratio. Relative, rather than absolute, mass flow rates are given because the sodium concentration was outside the range that could be run in the laboratory calibration apparatus.

Table 5.
Concentrations and Mass Flow Rates of Sodium at the Electrostatic Precipitator Outlet.

Run No.	O_2/n.g. v/v	Na Conc., μg/m³ ave.	Na Conc., μg/m³ std. dev.	Na Conc., μg/m³ low	Na Conc., μg/m³ high	Gas Flow actual m³/s	-- Na Flow, lb/hour -- ave.	-- Na Flow, lb/hour -- std. dev.	-- Na Flow, lb/hour -- low	-- Na Flow, lb/hour -- high
8	1.85	18	31	3	105	5.106	0.00073	0.00125	0.00012	0.00425
9	2.0	no sodium measurements during this run								
10	1.95	5.4	3.3	2	13	5.650	0.00025	0.00015	0.00009	0.00058
11	1.7	1.9	2.4	0	5	4.737	0.00007	0.00009	0	0.00019
12	1.6	17	40	0	107	4.729	0.00063	0.00150	0	0.00402
13	1.75	2.0	1.0	0.4	3.4	5.064	0.00008	0.00004	0.00002	0.00013
14	1.65	0.95	0.87	0	1.9	4.778	0.00004	0.00003	0	0.00007
15	1.7	3.4	7.4	0	18	4.729	0.00013	0.00028	0	0.00067
16	1.95	63	85	2	178	5.382	0.00269	0.00363	0.00009	0.00760
17	1.85	28	62	1	154	5.141	0.00114	0.00253	0.00004	0.00629

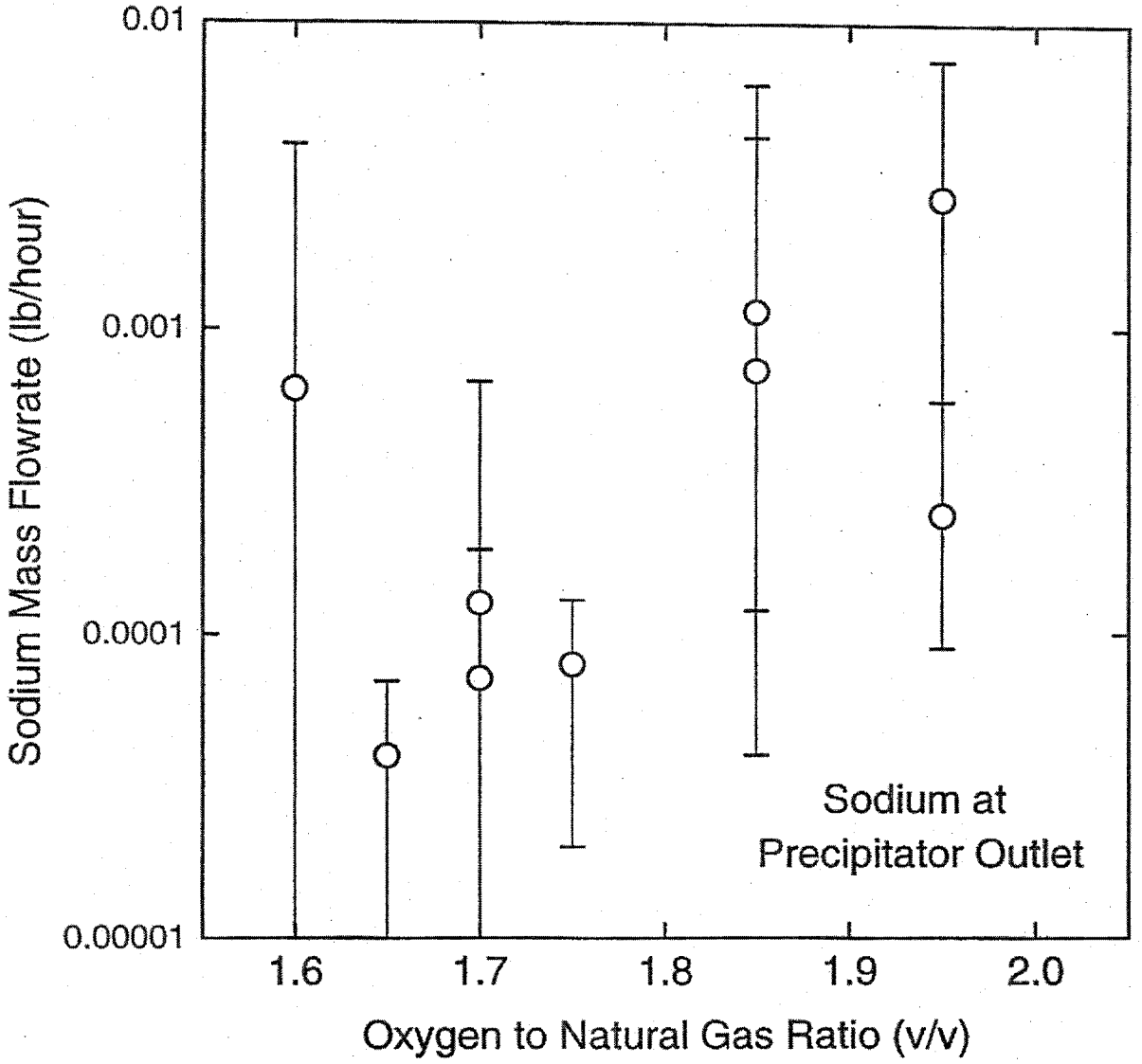

Figure 12. Dependence of sodium mass flow rate at the electrostatic precipitator outlet on oxygen to natural gas ratio. In this case the error bars indicate the maximum and minimum values recorded, not the standard deviation of the measurements as in the other figures.

The rate of caustic soda injection into the flue gas and the density of the solution are displayed on the monitors in the control room. The values were recorded during all of the runs when measurements were being made at the electrostatic precipitator outlet, but they are not included in Table 1 because there was no variation in the readings from run to run. The flow rate was 1 gal/min and the density 1.09 g/mL, corresponding to a NaOH concentration of 8.3 wt%. The sodium feed rate obtained from these data is 23.8 lb/hour. Based on this figure alone, neglecting any contribution to sodium from volatilization, and taking an approximate upper bound of 0.01 lb/hour on the sodium flow rate at the exit from the precipitator (Figure 12), one would conclude that the efficiency of the electrostatic precipitator for collection of sodium was greater than about 99.96%.

If we assume, because the sodium mass flow rate at the precipitator outlet was so low, that all of the boron observed there was present as metaboric acid, then, using the conversion factor from B to HBO_2 of 4.1 determined earlier and the average boron mass flow rate of 0.065 lb/hour at the oxygen to gas ratio of 1.85 (Table 3 and Figure 10), the contribution of metaboric acid to particulate matter at the precipitator outlet under this condition would have been 0.27 lb/hour.

CONCLUSIONS AND RECOMMENDATIONS

Conclusions

The influence of burner adjustment on volatilization and capture of boron and sodium were investigated in the range of oxygen to natural gas ratios from 1.6 to 2.0, from quite rich to approximately stoichiometric. The volatilization of boron, measured in units of total mass per unit time or units of mass per unit of melting area per unit time, was independent of the oxygen to natural gas ratio at the burners, to within approximately ± 7%, over this range of burner adjustment. Sodium volatilization, on the other hand, increased by approximately 40% over the same interval. The boron mass flow at the exit from the electrostatic precipitator decreased by 30% over the range of oxygen to gas ratios from 1.6 to 1.85 then increased slightly at the higher ratios of 1.95 and 2.0. Because the boron flow rate entering the precipitator was nearly independent of oxygen to gas ratio, the latter observation suggests that there was a maximum in the efficiency of the precipitator for collection of boron near the oxygen to gas ratio of 1.85, under the conditions investigated. The actual collection efficiency for boron could not be quantified because only relative values of boron concentration entering the precipitator were determined. The sodium flow from the electrostatic precipitator was highly variable, but below 0.01 lb/hour under all of the conditions at which data were obtained, over the range of oxygen to gas ratios from 1.6 to 1.95. A very conservative estimate placed the efficiency of the electrostatic precipitator for collection of sodium above 99.96%; it may be significantly higher.

The NO_X emission at an oxygen to natural gas ratio of 1.9 was 49.6 lb/hour; at a ratio of 1.85, it was 38 to 46 lb/hour. A minimum in the boron flow rate leaving the electrostatic precipitator was observed at the oxygen to gas ratio of 1.85. Under this condition the contribution of metaboric acid to particulate matter is estimated to have been only 0.27 lb/hour. From the point of view of NO_X and particulate matter emissions, the oxygen to gas ratio of 1.85, already identified as the baseline operating condition by the Chowchilla Plant engineers, appears to be very close to the true optimum.

An investigation of the spectrum of light emitted from the combustion space showed that emission from BO_2 at 547 nm was too weak to provide a measure of the spatial distribution of boron species in the combustion space. Emission lines characteristic of the alkali metals were observed, in order of their intensity: sodium, potassium, rubidium, and lithium. More sophisticated approaches, e.g. laser-induced fluorescence, to measurement of BO_2 are possible, but these should be investigated first in the laboratory.

Recommendations

The following are suggested as worthwhile extensions of the work.

1. The equilibrium vapor pressure of boron species under conditions in the electrostatic precipitator could be studied using one of the commercially available codes written specifically to handle solid and molten metal oxide mixtures and related systems. The objectives would be to answer the following questions:

a. Why is there an apparent increase in the collection efficiency for boron with increasing oxygen to gas ratio, in the absence of any significant change in the inlet or outlet gas temperatures? What are the optimum oxygen and carbon monoxide contents of the gas from the point of view of particulate removal?

b. What effects would increasing or decreasing the caustic soda feed rate have on the collection efficiency for boron?

c. Would decreasing the gas temperature at the entrance to the electrostatic precipitator be likely to make a significant improvement in collection efficiency?

2. A measurement campaign similar to the present one could be conducted, using LIBS to measure boron and sodium at the outlet from the electrostatic precipitator as functions of the caustic soda injection rate into the spray tower (suggestion by Jeffrey T. Curtin), to determine the optimum injection rate consistent with emissions limits. If this were done, the following should be taken into consideration:

a. The flow in the duct downstream from the electrostatic precipitator is not likely to have the profile characteristic of fully developed turbulent flow, so the use of the correlation of average and maximum velocities to estimate the volumetric flow rate from a single measurement at the centerline is questionable. A special Pitot/static probe should be obtained to measure the profiles of gas velocity in the duct along two perpendicular paths. Because the velocities here are low, the Pitot/static head is very low, so the best possible means of measuring the pressure difference should be identified.

b. An argument could be made that the concentration of the caustic soda should be decreased and the flow rate of solution increased, even if the injection rate of sodium hydroxide is not changed, if the cooling provided by additional water would have a beneficial effect on collection efficiency.

NOMENCLATURE

CCD	charge-coupled device (used to record the LIBS spectra)
DOE	U.S. Department of Energy
EP	electrostatic precipitator
in. w. c.	inches of water column
LIBS	laser-induced breakdown spectroscopy
n. g.	natural gas
OIT	the Office of Industrial Technologies in U.S. DOE
u	gas velocity, m/s
ΔP	Pitot/static pressure difference, Pa
ρ	gas density, kg/m^3

REFERENCES

Buckley, S. G., P. M. Walsh, D. W. Hahn, R. J. Gallagher, M. K. Misra, J. T. Brown, S. S. C. Tong, F. Quan, K. Bhatia, K. K. Koram, V. I. Henry, and R. D. Moore, "Measurements of Sodium in an Oxygen-Natural Gas Fired Soda-Lime-Silica Glass Melting Furnace," *60th Conference on Glass Problems*, J. Kieffer (Ed.), The American Ceramic Society, Westerville, OH, 2000, pp. 183-205.

Golubev, I. F., *Viscosity of Gases and Gas Mixtures: A Handbook*, Translated from the Russian by R. Kondor, D. Slutzkin (Ed.), Israel Program for Scientific Translations, Jerusalem, 1970, Chapters IV and VI.

Green, D. W., and J. O. Maloney (Eds.), *Perry's Chemical Engineers' Handbook*, 6th edition, McGraw-Hill, New York, 1984, Fig. 5-14, p. 5-12.

Slade, S. J., "Glass Furnace Waste Gas Chemistry," in: *Corrosion of Materials by Molten Glass, Ceramic Transactions*, Vol. 78, G. A. Pecoraro, J. C. Marra, and J. T. Wenzel (Eds.), American Ceramic Society, Westerville, OH, 1996, pp. 195-204.

Walsh, P. M., and R. D. Moore, "Na Vapor and Gas Temperature Measured in Glass Container Furnaces," *the GlassResearcher: Bulletin of Glass Science and Engineering*, Vol. 10, No. 1, 2000, pp. 6-8.

APPENDIX A

Semi-quantitative analysis of electrostatic precipitator dust sample collected on July 18, 2000.

Semi-quantitative analysis of slag from the vertical flue collected on July 18, 2000.

Quantitative analysis of electrostatic precipitator dust sample collected on August 31, 2000.

LABORATORY ANALYSIS REPORT

CELS Client No.: 275163-002

Exhibit A : Semi-Quantitative Spectrographic Analysis

Sample Description:

Sample 1: CT-1 EP Dust from Borosilicate Melting Furnace; 7-18-00

Folder No.: 40493-00

RESULTS (Reported As The ***"ELEMENT"***)

Range(Wt%)	
>30	Na
10-30	-
3.0-10	B
1.0-3.0	K,Si
0.3-1.0	Ca,Cr-
0.1-0.3	Al,Mg
0.03-0.1	-
0.01-0.03	Fe,Mn,Pb,Sn
0.003-0.01	Ba,Bi,Ti
0.001-0.003	-
<0.001	Cu,Sr

An element may appear in a semi-quantitative range that is one range higher or one range lower than its actual concentration.
Typical detection limits (Wt%) for the ELEMENTS EXAMINED are listed below. They are ONLY general guidelines. Detection limits are composition affected.

1.0%	- K	0.01%	- Ba,Na,Sb,Zr
0 .3%	- P	0.003%	- Al,Ca,Co,In,Ni,Si,Ti
0.1%	- As,Cd,Li	0.001%	- Ag,B,Be,Bi,Cu,Cr,Fe,Ga,Mg,Mn,Mo,Pb,Sn,Sr,V
0.03%	- Nb,Zn		

[(+) = Upper Range, (-) = Lower Range, (?) = Possibly Present]

ANALYSIS COMMENT:

CONFIDENTIAL: This CELS report information is to be used only for account 275163.

LABORATORY ANALYSIS REPORT

CELS Client No.: 275163-003

Exhibit A : Semi-Quantitative Spectrographic Analysis

Sample Description:

Sample 1: CT-2 Slag from flue of borosilicate glass melting furnace; 7-18-00

Folder No.: 40776-00

RESULTS (Reported As The ***"ELEMENT"***)

Range(Wt%)	
>30	-
10-30	B-,Na,Si
3.0-10	Al
1.0-3.0	Ca,Cr,Mg
0.3-1.0	K,Zr
0.1-0.3	Fe,Sb
0.03-0.1	As,Co,Mn,Pb+
0.01-0.03	Sn+,Ti
0.003-0.01	Ba,Bi,Cu-
0.001-0.003	Ag-,Ga,Ni,Sr
<0.001	V

An element may appear in a semi-quantitative range that is one range higher or one range lower than its actual concentration.
Typical detection limits (Wt%) for the ELEMENTS EXAMINED are listed below. They are ONLY general guidelines. Detection limits are composition affected.

1.0%	- K	0.01%	- Ba,Na,Sb,Zr
0 .3%	- P	0.003%	- Al,Ca,Co,In,Ni,Si,Ti
0.1%	- As,Cd,Li	0.001%	- Ag,B,Be,Bi,Cu,Cr,Fe,Ga,Mg,Mn,Mo,Pb,Sn,Sr,V
0.03%	- Nb,Zn		

[(+) = Upper Range, (-) = Lower Range, (?) = Possibly Present]

ANALYSIS COMMENT: Li was not tested for. Li may be present.

CONFIDENTIAL: This CELS report information is to be used only for account 275163.

LABORATORY ANALYSIS REPORT

CELS Client No.: 275163-003

Exhibit A : Semi-Quantitative Spectrographic Analysis (Continued)

BELOW is a list of the ELEMENTS that are determined by spectrographic analysis. Analyses are divided into three categories: **GENERAL QUANTITATIVE, NOBLE METALS**, AND **RARE EARTHS.**

Analysis for the Noble Metals and/or Rare Earths must be requested, if needed. They are not part of the General Quantitative Analysis. They can be requested by the group or by the element of interest.

GENERAL QUANTITATIVE ANALYSIS Ag, Al, As, B, Ba, Be, Bi, Ca, Cd, Ce, Co, Cr, Cu, Fe, Ga, Ge, In, K, Mg, Mn, Mo, Na, Nb, Ni, P, Pb, Sb, Si, Sn, Sr, Ti, V, Zn, Zr. (If requested) Ta-0.1%, Te-0.1%, Tl-0.01%, W-0.3-1%

NOBLE METALS ANALYSIS

ELEMENT	DETECTION %
Au	0.003
Ga	0.001
Hf	0.1
In	0.001
Ir	0.01
Pd	0.001
Pt	0.01
Re	0.03
Rh	0.001
Ru	0.03

RARE EARTHS ANALYSIS

ELEMENT	DETECTION %	ELEMENT	DETECTION%
Ce	0.1	Nd	0.3
Dy	0.1	Pr	0.1
Er	0.1	Sc	0.01
Eu	0.01	Sm	0.1
Gd	0.03	Tb	0.03
Ho	0.03	Tm	0.01
La	0.1	Y	0.003
Lu	0.01	Yb	0.001

Semi-Quantitative Spectrographic Analysis RESULTS are reported as weight percent of the **ELEMENT** (NOT as the oxide). To convert weight percent element to weight percent oxide, MULTIPLY the percent element by the appropriate factor listed in the table below.

FACTORS FOR CONVERSION

Ag2O	1.07	Eu2O3	1.16	MoO3	1.50	SrO	1.18
Al2O3	1.89	FeO	1.29	Na2O	1.35	Ta2O5	1.22
As2O3	1.32	Fe2O3	1.43	Nb2O5	1.43	Tb4O7	1.18
As2O5	1.53	Ga2O3	1.34	Nd2O3	1.17	TeO2	1.25
B2O3	3.22	Gd2O3	1.15	NiO	1.27	TiO2	1.67
BaO	1.12	GeO2	1.44	P2O5	2.29	Tl2O	1.04
BeO	2.78	PbO	1.08	PbO2	1.15	Tl2O3	1.12
Bi2O3	1.11	Ho2O3	1.15	Pr2O3	1.17	Tm2O3	1.14
CaO	1.40	HfO2	1.18	RuO4	1.63	VO	1.31
CdO	1.14	In2O3	1.12	RuO2	1.32	VO2	1.63
CeO2	1.23	K2O	1.20	Sb2O3	1.20	V2O5	1.79
Co3O4	1.36	La2O3	1.17	Sb2O5	1.33	WO2	1.17
Cr2O3	1.46	Li2O	2.15	Sc2O3	1.53	WO3	1.26
CuO	1.25	Lu2O3	1.14	SiO2	2.14	Y2O3	1.27
Cu2O	1.13	MgO	1.66	Sm2O3	1.16	Yb2O3	1.14
Dy2O3	1.15	MnO	1.29	SnO	1.13	ZnO	1.24
Er2O3	1.14	MnO2	1.58	SnO2	1.27	ZrO2	1.35

CONFIDENTIAL: This CELS report information is to be used only for account 275163.

LABORATORY ANALYSIS REPORT

CELS Client No.: 275163-004

Exhibit A : Quantitative Chemical Analysis

Sample Description:
Sample 1: CA-3 Dust from Electrostatic Precipitation of Borosilicate Glass Melting Furnace; 8-31-00
Folder No.: 42680-00

Oxide	Sample 1 (Wt%)	Test Method
Cr_2O_3	0.55	AAS
MnO_2	0.054	AAS
K_2O	5.61	FES
Li_2O	<0.01	FES
Na_2O	35.7	FES
Rb_2O	<0.01	FES
Al_2O_3	0.24	ICP
B_2O_3	24.8	ICP
CaO	0.95	ICP
Fe_2O_3 (1)	0.055	ICP
MgO	0.46	ICP
SiO_2	4.69	ICP
TiO_2	0.009	ICP
ZrO_2	0.004	ICP
O_2	32.0	LECO
C	2.8	LECO
SO_3	17	LECO
LOD	0.89	LOD
LOI	13.8	LOI
Cl	1.26	TITR

(1) Total Fe expressed as Fe_2O_3

Legend:
AAS: Atomic Absorption Spectroscopy
FES: Flame Emission Spectroscopy
ICP: Inductively Coupled Plasma Spectroscopy
LECO: LECO (R) Instrumentation
LOD: Loss On Drying At 110oC
LOI: Loss on Ignition at 1000oC
TITR: Titrimetry

CONFIDENTIAL: This CELS report information is to be used only for account 275163.

LABORATORY ANALYSIS REPORT

CELS Client No.: 275163-004

Exhibit A: Quantitative Chemical Analysis

NOTE: The methodology used measures the elemental concentration. The results are reported in oxide form.

Accuracy Statement

The following is a guideline of the accuracy of the Atomic Spectroscopy chemical analysis.

The actual accuracy depends on the specific element and the matrix of the material being analyzed. Also, the approximate composition of the material is required to achieve this accuracy.

Major Components - Levels >2%:

Accuracy is generally +/- 0.5 to 1, relative % of absolute value.

i.e. for a level of 30.0%, the absolute standard deviation will range between 0.15% and 0.30%

Minor Components - Levels between 0.5% to 2.0%:

Accuracy is +/- 1 to 5, relative % of absolute value.

Note: The relative error will be less as the value approaches the 2% level.

i.e. for a level of 1.0%, the absolute standard deviation will range between 0.01% and 0.05%

Minor to Trace Components - Levels < 0.5%:

Accuracy is +/- 2 to 20, relative % of absolute value.

Note: The relative error will be higher as the value approaches trace levels..

i.e. for a level of 0.1%, the absolute standard deviation will range between 0.002% and 0.02%

CONFIDENTIAL: This CELS report information is to be used only for account 275163.

APPENDIX B

Analyses of the natural gas and the fuel oil used to wet the batch.

Yosemite Division Account Services
3185 M Street
Merced, CA 95348

Natural Gas Composition Analysis

RESULTS FOR LAST CYCLE — DATE 08/08/2000
Stream #: 1 (Herndon Jct T04)

COMPONENT NAME	MOLE %
1. N-HEXANE & N-HEPTANE (C^6)	0.010
2. PROPANE (C^3)	0.182
3. ISO-BUTANE (IC^4)	0.021
4. N-BUTANE & NEO-PENTANE (NC^4)	0.031
5. ISO-PENTANE (IC^5)	0.011
6. N-PENTANE (NC^5)	0.005
7. NITROGEN (N^2)	1.61
8. METHANE (C^1)	95.33
9. CARBON DIOXIDE (CO^2)	1.11
10. ETHANE (C^2)	1.60

BTU for last cycle	1004.8
Specific Gravity for Last Cycle	0.5836
Compressibility for Last Cycle	0.9976
Unnormalized Total for Last Cycle	96.84%

Peter Walsh
Sandia National Laboratories
mail Stop 9051

Livermore, CA 94551

Date: September 17, 2000
REQUEST NUMBER: 17538
LAB NUMBER: G9490

SAMPLE ID:
CA-4 8-31-00

REPORT OF ANALYSIS

CARBON, wt %	78.51
HYDROGEN, wt %	21.45
NITROGEN, wt %	0.01
SULFUR, wt %	0.01
ASH, wt %	0.01
OXYGEN, wt %	0.01
TOTAL	100.00
MOISTURE, vol %	< 0.1
SPECIFIC GRAVITY, 60F/60F	0.830
API	39.0
DENSITY, lb/gal	6.93

Fuel Oil Analysis

Monte L. Ellis

Monte L. Ellis
Laboratory Manager

MLE:tab

WYOMING ANALYTICAL LABORATORIES, INC.
1660 Harrison St.
Laramie, WY 82070
wallaramie@aol.com
(307) 742-7995
Fax: (307) 721-8956
MEMBER ACIL

APPENDIX C

Computer code for calculation of the volumetric flow rate of gas from a Pitot/static pressure measurement on the centerline of a fully-developed flow in a circular flue duct, based upon knowledge of the natural gas, oxygen, batch, cullet, fuel oil, water, and caustic soda feeds and their compositions, but in the presence of an unknown total flow rate of bubblers, camera cooling, spray atomization, and inleaking air.

```
//This program calculates the flowrate and composition of flue gas from
//the CertainTeed borosilicate glass melting tank at Chowchilla, CA.

#include <stdio.h>
#include <math.h>
#include <stdlib.h>

#define R 8314.51    //universal gas constant, J/kmol.K
#define PSTD 101325.    //standard pressure, Pa
#define TSTD 293.15    //standard temperature, 68 deg F
#define WH 1.007940    //atomic weights, kg/kmol
#define WC 12.011
#define WN 14.00674
#define WO 15.9994
#define WAr 39.948
#define PI  3.1415927

double rhog;    //flue gas density, kg/m3
double Tg;      //gas temperature, K
double XN2ng, XCO2ng, XC1ng, XC2ng, XC3ng, XC4ng, XC5ng, XC6ng;    //mole fractions, dimensionless
double mug;     //viscosity of flue gas, kg/m.s
double Wg;      //average molecular weight of flue gas, kg/kmol
double Re;      //duct Reynolds number, dimensionless
double WH2O = 2. * WH + WO;  // molecular weights
double WCO2 = WC + 2. * WO;
double WN2 = 2. * WN;
double WO2 = 2. * WO;
double WC1 = WC + 4. * WH;
double WC2 = 2. * WC + 6. * WH;
double WC3 = 3. * WC + 8. * WH;
double WC4 = 4. * WC + 10. * WH;
double WC5 = 5. * WC + 12. * WH;
double WC6 = 6. * WC + 14. * WH;
double m3PERft3, Cg, Cgstd, kgPERlb, Wng, fng, fox, fair, FH2O, nng, nO2, nox;
double ntotal, vtotal, XO2air, PaPERinwater, Pbar, Pg, fH2O, nH2Oquench, nH2O;
double XH2O, XCO2, XO2, XN2, Aduct, dPitot, vPitot, nCO2, nCO2comb, nH2Ocomb;
double XO2ox, nN2, nAr, XAr, Xtotal, ffluegas, nO2comb, oxngstoich, O2deficit;
double velratio, ugave, ugmax, fglass, fbatch, rglassbatch, nH2Obatch, YH2Obatch;
double YCO2batch, nCO2batch, Tamb, relhum, Dduct, XArox, ntotaldry, XO2dry;
double fcaustic, YHoil, YCoil, arg1, arg2, PH2Oambeq, rhooil, PH2Oair, XH2Oair;
double nH2Oair, nairwet, nairdry, foil, roilbatch, nHoil, nCoil, vairstd, XO2drymeas;
double mui, muj, muO2, muAr, muCO2, muH2O, muN2, ni, nj, Wi, Wj, sumi, phiij;
double XArair, XCO2air, Z;

void main(void)
{
   //Conversion factors and Constants
   m3PERft3 = pow((1. / (0.0254 * 12.)), 3.);
   Cgstd = PSTD / (R * TSTD);  //kmol/m3
   kgPERlb = 0.4536;
```

```
XO2air = 0.20946 ;
PaPERinwater = 248.2104 ;  //water at 22 deg C (Meriam Instrument data sheet)
YH2Obatch =        ;
YCO2batch =        ;
rglassbatch = 1. - YH2Obatch - YCO2batch ;   //ratio glass pull to batch feed rate
XArox = 0.0446 ;   //Assume all argon in air retained in the oxygen
XArair = 0.00934 ;    //mole fraction argon in dry air
XCO2air = 365.e-6 ;    //mole fraction carbon dioxide in dry air

//Fixed furnace conditions
fglass =      ;   //metric ton/day
fglass = fglass * 1000. / (24. * 3600.);
fbatch = fglass / rglassbatch ;
ffluegas =        ;  //Jeff Curtin's estimate of actual flue gas flowrate
ffluegas = ffluegas / (60. * m3PERft3 );   //actual m^3/s

//Natural Gas Composition, mole fractions
XC1ng = 0.9533 ;
XC2ng = 0.0160 ;
XC3ng = 0.00182 ;
XC4ng = 0.00052 ;
XC5ng = 0.00016 ;
XC6ng = 0.00010 ;
XCO2ng = 0.0111 ;
XN2ng = 0.0161 ;
Wng =  WC1 * XC1ng + WC2 * XC2ng + WC3 * XC3ng + WC4 * XC4ng + WC5 * XC5ng + WC6 * XC6ng + WCO2 * XCO2ng + WN2 * XN2
Z = 0.9976 ;    //compressibility factor

//Batch oil composition and elemental flowrates
YHoil = 0.2145 ;    //Wyoming Analytical Laboratories' analysis, 9/17/2000.
YCoil = 0.7851 ;    //                          "
rhooil = 6.93 ;     //pounds per gallon,  "
roilbatch =    * rhooil /        ;
foil = fbatch * roilbatch ;   //kg/s
nHoil = foil * YHoil / WH;     //kmol/s
nCoil = foil * YCoil / WC;     //kmol/s

//Duct diameter and area
Dduct = 41.;                          //inches
Dduct = Dduct * 0.0254 ;
Aduct = PI * pow(Dduct, 2.) / 4.;

//Enter Data
printf ("Enter the ambient temperature, deg F:    "   );
scanf ("%lf", &Tamb);
Tamb = (Tamb + 459.67) * 5. / 9.;
printf ("Enter the barometric pressure, mm Hg:    "   );
scanf ("%lf", &Pbar);
Pbar = Pbar * PSTD / 760.;
printf ("Enter the relative humidity, %:    "   );
```

```
scanf("%lf", &relhum);
printf("Enter the oxygen purity, %:    ");
scanf("%lf", &XO2ox);
XO2ox = XO2ox / 100.;
printf("Enter the oxygen flowrate, kscfh:    ");
scanf("%lf", &fox);
fox = fox * 1000.;
printf("Enter the natural gas flowrate, kscfh:    ");
scanf("%lf", &fng);
fng = fng * 1000.;
printf("Enter the duct pressure, Pa, negative:    ");
scanf("%lf", &Pg);
Pg = Pbar - Pg;
printf("Enter the Pitot/static differential pressure, Pa:    ");
scanf("%lf", &dPitot);
dPitot = dPitot * (1. + 0.0007 * (293.15 - Tamb));
printf("Enter the flue gas temperature, deg F:    ");
scanf("%lf", &Tg);
Tg = (Tg + 459.67) * 5. / 9.;
printf("Enter the quench water flowrate, gallon/minute:    ");
scanf("%lf", &fH2O);
printf("Enter the caustic soda flowrate, gallon/minute:    ");
scanf("%lf", &fcaustic);
fH2O = fH2O + fcaustic;

//Mole fraction water in ambient air, correlation from Keenan and Keyes, 1936, p. 14.
//(might be improved by using more recent values for the critical pressure and temperature,
//but the constants below are more than sufficiently accurate for present purposes)
arg1 = 647.27 - Tamb;
arg2 = - (arg1 / Tamb) * ((3.2437814 + (5.86826e-3 * arg1) + (1.1702379e-8 * pow(arg1, 3.))) / (1. + 2.1878462e-3 *
1));
PH2Oambeq = 218.167 * pow(10., arg2);      //atmospheres
PH2Oambeq = PH2Oambeq * PSTD;     //Pascal
PH2Oair = PH2Oambeq * relhum / 100.;
XH2Oair = PH2Oair / Pbar;

//Feed Rates
fair = 0.5;  //std. m3/s
vPitot = 1.;
vtotal = 0.;

while (fabs(vPitot - vtotal) > 0.0001)
{
fair = fair + 0.00005;
nng = (fng /(m3PERft3 * 3600.)) * (Cgstd / Z);  //kmol/s
nox = (fox /(m3PERft3 * 3600.)) * Cgstd;  //kmol/s
nairwet = fair * Cgstd;  //kmol/s
nairdry = nairwet * (1. - XH2Oair);
nH2Oair = nairwet * XH2Oair;
nH2Oquench = fH2O * 8. * kgPERlb / (60. * WH2O);  //kmol/s
```

```
nH2Obatch = fbatch * YH2Obatch / WH2O;
nCO2batch = fbatch * YCO2batch / WCO2;

//Calculate Flowrates of Combustion Products, Excess Oxygen, and Excess Air
nCO2comb = nng * (XC1ng * 1. + XC2ng * 2. + XC3ng * 3. + XC4ng * 4. + XC5ng * 5. + XC6ng * 6.) + nCoil;
nH2Ocomb = nng * (XC1ng * 2. + XC2ng * 3. + XC3ng * 4. + XC4ng * 5. + XC5ng * 6. + XC6ng * 7.) + 0.5 * nHoil;
nO2comb = nCO2comb + 0.5 * nH2Ocomb;
O2deficit = (nO2comb - nox * XO2ox) / (nox * XO2ox);
oxngstoich = nO2comb / (XO2ox * nng);
nO2 = nairdry * XO2air + nox * XO2ox - nO2comb;
if(XO2ox < (1. - XArox)){
   nN2 = nairdry * (1. - XO2air - XArair - XCO2air) + nox * (1. - XO2ox - XArox) + nng * XN2ng;
   nAr = nox * XArox + nairdry * XArair;
   }
else{
   nN2 = nairdry * (1. - XO2air - XArair - XCO2air) + nng * XN2ng;
   nAr = nox * (1. - XO2ox) + nairdry * XArair;
   }

//Calculate Flue Gas Flowrate from Feeds
nH2O = nH2Ocomb + nH2Oquench + nH2Obatch + nH2Oair;
nCO2 = nCO2comb + nng * XCO2ng + nCO2batch + nairdry * XCO2air;
ntotal = nH2O + nCO2 + nO2 + nN2 + nAr;
ntotaldry = nCO2 + nO2 + nN2 + nAr;
Cg = Pg / (R * Tg);
vtotal = ntotal / Cg;

//Calculate the Flue Gas Composition
XH2O = nH2O / ntotal;
XCO2 = nCO2 / ntotal;
XO2 = nO2 / ntotal;
XO2dry = nO2 / ntotaldry;
XN2 = nN2 / ntotal;
XAr = nAr / ntotal;
Xtotal = XH2O + XCO2 + XO2 + XN2 + XAr;

//Calculate flue gas molecular weight and density
Wg = (XH2O * WH2O) + (XN2 * WN2) + (XCO2 * WCO2) + (XO2 * WO2) + (XAr * WAr);   //average molecular weight
rhog = Pg * Wg / (R * Tg);   //density of gas, kg/m3

//Calculate gas mixture viscosity

muN2 = 1.392e-6 * pow(Tg, 1.5) / (Tg + 104.7);  //viscosity of nitrogen, kg/m.s
muH2O = 1.e-7 * (0.361 * Tg - 10.2);  //viscosity of steam, Tg < 800 K, Hilsenrath, kg/m.s
muCO2 = 1.600198e-6 * pow(Tg, 1.5) / (Tg + 254.);
muO2 = 1.69567e-6 * pow(Tg, 1.5) / (Tg + 125.);  //15 - 630 degC, Golubev and Kestin and Wakeham
muAr = 1.93393e-6 * pow(Tg, 1.5) / (Tg + 142.);   //20 - 827 degC, Golubev and Kestin and Wakeham
mug = 0.;

//Contribution from nitrogen
```

```
if(XN2 == 0)
   mug += 0.;
else {
mui = muN2;
ni = XN2;
Wi = WN2;
sumi = 0.;
muj = muH2O;
nj = XH2O;
Wj = WH2O;
phiij = pow(2., 0.5) * pow((1. + (pow(mui/muj, 0.5) * pow(Wj/Wi, 0.25))), 2.)/(4. * pow((1.+(Wi/Wj)), 0.5));
sumi = sumi + (nj * phiij);
muj = muCO2;
nj = XCO2;
Wj = WCO2;
phiij = pow(2., 0.5) * pow((1. + (pow(mui/muj, 0.5) * pow(Wj/Wi, 0.25))), 2.)/(4. * pow((1.+(Wi/Wj)), 0.5));
sumi = sumi + (nj * phiij);
muj = muO2;
nj = XO2;
Wj = WO2;
phiij = pow(2., 0.5) * pow((1. + (pow(mui/muj, 0.5) * pow(Wj/Wi, 0.25))), 2.)/(4. * pow((1.+(Wi/Wj)), 0.5));
sumi = sumi + (nj * phiij);
muj = muAr;
nj = XAr;
Wj = WAr;
phiij = pow(2., 0.5) * pow((1. + (pow(mui/muj, 0.5) * pow(Wj/Wi, 0.25))), 2.)/(4. * pow((1.+(Wi/Wj)), 0.5));
sumi = sumi + (nj * phiij);
mug += mui /(1. + (sumi / ni));
}

//Contribution from steam
if(XH2O == 0)
   mug += 0.;
else {
mui = muH2O;
ni = XH2O;
Wi = WH2O;
sumi = 0.;
muj = muN2;
nj = XN2;
Wj = WN2;
phiij = pow(2., 0.5) * pow((1. + (pow(mui/muj, 0.5) * pow(Wj/Wi, 0.25))), 2.)/(4. * pow((1.+(Wi/Wj)), 0.5));
sumi = sumi + (nj * phiij);
muj = muCO2;
nj = XCO2;
Wj = WCO2;
phiij = pow(2., 0.5) * pow((1. + (pow(mui/muj, 0.5) * pow(Wj/Wi, 0.25))), 2.)/(4. * pow((1.+(Wi/Wj)), 0.5));
sumi = sumi + (nj * phiij);
muj = muO2;
nj = XO2;
```

```
Wj = WO2;
phiij = pow(2., 0.5) * pow((1. + (pow(mui/muj, 0.5) * pow(Wj/Wi, 0.25))), 2.)/(4. * pow((1.+(Wi/Wj)), 0.5));
sumi = sumi + (nj * phiij);
muj = muAr;
nj = XAr;
Wj = WAr;
phiij = pow(2., 0.5) * pow((1. + (pow(mui/muj, 0.5) * pow(Wj/Wi, 0.25))), 2.)/(4. * pow((1.+(Wi/Wj)), 0.5));
sumi = sumi + (nj * phiij);
mug += mui /(1. + (sumi / ni));
}

//Contribution from oxygen
if(XO2 == 0)
   mug += 0.;
else {
mui = muO2;
ni = XO2;
Wi = WO2;
sumi = 0.;
muj = muH2O;
nj = XH2O;
Wj = WH2O;
phiij = pow(2., 0.5) * pow((1. + (pow(mui/muj, 0.5) * pow(Wj/Wi, 0.25))), 2.)/(4. * pow((1.+(Wi/Wj)), 0.5));
sumi = sumi + (nj * phiij);
muj = muCO2;
nj = XCO2;
Wj = WCO2;
phiij = pow(2., 0.5) * pow((1. + (pow(mui/muj, 0.5) * pow(Wj/Wi, 0.25))), 2.)/(4. * pow((1.+(Wi/Wj)), 0.5));
sumi = sumi + (nj * phiij);
muj = muN2;
nj = XN2;
Wj = WN2;
phiij = pow(2., 0.5) * pow((1. + (pow(mui/muj, 0.5) * pow(Wj/Wi, 0.25))), 2.)/(4. * pow((1.+(Wi/Wj)), 0.5));
sumi = sumi + (nj * phiij);
muj = muAr;
nj = XAr;
Wj = WAr;
phiij = pow(2., 0.5) * pow((1. + (pow(mui/muj, 0.5) * pow(Wj/Wi, 0.25))), 2.)/(4. * pow((1.+(Wi/Wj)), 0.5));
sumi = sumi + (nj * phiij);
mug += mui /(1. + (sumi / ni));
}

//Contribution from carbon dioxide
if(XCO2 == 0)
   mug += 0.;
else {
mui = muCO2;
ni = XCO2;
Wi = WCO2;
sumi = 0.;
```

```
muj = muH2O;
nj = XH2O;
Wj = WH2O;
phiij = pow(2., 0.5) * pow((1. + (pow(mui/muj, 0.5) * pow(Wj/Wi, 0.25))), 2.)/(4. * pow((1.+(Wi/Wj)), 0.5));
sumi = sumi + (nj * phiij);
muj = muN2;
nj = XN2;
Wj = WN2;
phiij = pow(2., 0.5) * pow((1. + (pow(mui/muj, 0.5) * pow(Wj/Wi, 0.25))), 2.)/(4. * pow((1.+(Wi/Wj)), 0.5));
sumi = sumi + (nj * phiij);
muj = muO2;
nj = XO2;
Wj = WO2;
phiij = pow(2., 0.5) * pow((1. + (pow(mui/muj, 0.5) * pow(Wj/Wi, 0.25))), 2.)/(4. * pow((1.+(Wi/Wj)), 0.5));
sumi = sumi + (nj * phiij);
muj = muAr;
nj = XAr;
Wj = WAr;
phiij = pow(2., 0.5) * pow((1. + (pow(mui/muj, 0.5) * pow(Wj/Wi, 0.25))), 2.)/(4. * pow((1.+(Wi/Wj)), 0.5));
sumi = sumi + (nj * phiij);
mug += mui /(1. + (sumi / ni));
}

//Contribution from argon
if(XCO2 == 0)
   mug += 0.;
else {
mui = muAr;
ni = XAr;
Wi = WAr;
sumi = 0.;
muj = muH2O;
nj = XH2O;
Wj = WH2O;
phiij = pow(2., 0.5) * pow((1. + (pow(mui/muj, 0.5) * pow(Wj/Wi, 0.25))), 2.)/(4. * pow((1.+(Wi/Wj)), 0.5));
sumi = sumi + (nj * phiij);
muj = muN2;
nj = XN2;
Wj = WN2;
phiij = pow(2., 0.5) * pow((1. + (pow(mui/muj, 0.5) * pow(Wj/Wi, 0.25))), 2.)/(4. * pow((1.+(Wi/Wj)), 0.5));
sumi = sumi + (nj * phiij);
muj = muO2;
nj = XO2;
Wj = WO2;
phiij = pow(2., 0.5) * pow((1. + (pow(mui/muj, 0.5) * pow(Wj/Wi, 0.25))), 2.)/(4. * pow((1.+(Wi/Wj)), 0.5));
sumi = sumi + (nj * phiij);
muj = muCO2;
nj = XCO2;
Wj = WCO2;
phiij = pow(2., 0.5) * pow((1. + (pow(mui/muj, 0.5) * pow(Wj/Wi, 0.25))), 2.)/(4. * pow((1.+(Wi/Wj)), 0.5));
```

```
    sumi = sumi + (nj * phiij);
    mug += mui /(1. + (sumi / ni));
    }

    //Calculate Flue Gas Flowrate from the Pitot/static Pressure Difference on the Centerline
    ugmax = pow((2. * dPitot / rhog), 0.5);
    Re = rhog * ugmax * Dduct / mug;
    velratio = 0.0325 * log10(Re) + 0.665;
    ugave = velratio * ugmax;
    vPitot = ugave * Aduct;
    }

    //Calculate air as difference
    vairstd = (vPitot - vtotal) * (TSTD / Tg) * (Pg / PSTD);

    //Display Results
    printf("\nThe oxygen deficit is:   %7.1lf %"   , O2deficit * 100.);
    printf("\nThe stoichiometric oxygen to gas ratio is:   %7.4lf"    , oxngstoich);
    printf("\nThe oxygen mole fraction, dry, is:   %7.4lf"    , XO2dry);
    printf("\nThe oxygen mole fraction, wet, is:   %7.4lf"    , XO2);
    printf("\nThe steam mole fraction is:   %7.4lf"    , XH2O);
    printf("\nThe carbon dioxide mole fraction, wet, is:   %7.4lf"    , XCO2);
    printf("\nThe nitrogen mole fraction, wet, is:   %7.4lf"    , XN2);
    printf("\nThe argon mole fraction, wet, is:   %7.4lf"    , XAr);
    printf("\nThe sum of the mole fractions is:   %7.4lf"    , Xtotal);
    printf("\nThe duct Reynolds number based on the maximum velocity is:   %10.0lf"    , Re);
    printf("\nThe ratio of average to centerline velocities is:   %7.4lf"    , velratio);
    printf("\nThe actual volumetric flow rate from Jeff Curtin is:  %7.3lf m^3/s"    , ffluegas);
    printf("\nThe actual volumetric flow rate from the feeds is:  %7.3lf m^3/s"    , vtotal);
    printf("\nThe air flowrate, at STP, needed to equate the two flowrates, is:  %7.4lf m3/s"    , vairstd);
    printf("\nThe calculated volumetric flowrate of air, at STP, is:  %7.4lf m3/s"    , fair);
    printf("\nThe corrected flowrate of air is:  %7.4lf m3/s"    , fair + vairstd);
    printf("\nThe actual volumetric flow rate from the gas velocity is:  %7.3lf m^3/s"    , vPitot);
}
```